Article

Biofilm early stages of growth and accumulation theoretical model

José M. Carvalho [a, b] , Manuel J. T. Carrondo [a, c, d] and Luis L. Bonilla [b, e]

a, LAQV-REQUIMTE, Chemistry Department, NOVA School of Science and Technology, Quinta da Torre, 2829-516 Caparica, Portugal

b, Escuela Politécnica Superior, Universidad Carlos III de Madrid, Butarque 15, 28911 Leganés, Spain

c, Instituto de Biologia Experimental e Tecnológica (IBET), Apartado 12, 2781 - 901 Oeiras, Portugal

d, Instituto de Tecnologia Química e Biológica (ITQB), Universidade Nova de Lisboa, Apartado 127, 2781 - 901 Oeiras, Portugal

e, Instituto Gregorio Millan, Escuela Politecnica Superior, Universidad Carlos III de Madrid, Avda. de la Universidad 30, Leganes 28911, Spain

*Correspondence: jmprc@fct.unl.pt;

Abstract: A theoretical model to translate the evolution over time, in early stages, of growth and accumulation of biofilm bacterial mass is introduced. The model implies the solution of a system of differential-difference master equations.

The application of an algorithm like Miller´s tree term recurrence, already known for Bessel functions of first kind, allows an exact calculation of the solutions of such equations, for a wide range of parameters values and time.

For biofilm model a five term recurrence is deduced and applied in a backwards computation. A suitable normalisation condition completes the reach of the solution.

Keywords: biofilm, Miller recurrent algorithm, Bessel functions, differential-difference master equations.

1. Introduction

Discrete mathematical models in space, and continuous in time, arise in many different contexts of Physics, Chemistry and Engineering. Ever since, consideration of more sophisticated exact mathematical solutions, for transient regimes, invariantly leads, in known bibliography, to numerical and approximated methods application. Such approach neglects all the theoretical information contained in an exact solution, which usually consists of special functions or, more frequently, complex combinations between them (in particular an infinite sum of terms with Bessel functions of first kind, modified or not).

As a matter of fact the accurate calculation of special functions seems far from being an inviting task in several fields of exact sciences, namely Operational Research [1,2], Teletraffic Theory [3] and Manufacturing Systems [4]. The commentary in [2] and subsequent ones, with the same inspiration,   many years after [5], and even nearly nowadays [6] corroborate such difficulties. Functions similar to that of transient M/M/1 queue also came into play in Physical-Chemistry (nucleation, polymerization, crystallization, ... , aggregation processes in general), in Radar Theory [7], in Computer Networks Theory [8], and Congestion phenomenon [9].

From those exact solutions little information is brought to light, with the exception of long time behaviour (steady state) which is a limit more easy to deduce. If transient regime is considered, having already an exact solution, a formalism of type Fokker-Planck is usually chosen to approximate such regime. The purpose is to mimic a process discrete in space and continuous in time by a process continuous both in space and time.

Doing things like that the initial infinite system of differential-difference equations is transformed in an equation with partial derivatives (Fokker-Planck equation). On the other hand special functions, that are the most important part of the solution, are eliminated from all the analysis, and so we lose all their formal beauty.

Formalism conducting to Fokker-Planck equation started when Frenkel brought Becker-Doring theoretical work on nucleation kinetics to "its modern form", as Goodrich said [10]. Seems that such "modern form", or others similar approximations, has been generally accepted in many domains of scientific knowledge already cited.

In recent years a theoretical model to account quantitatively the evolution over time of growth and accumulation of biofilm biomass lead to a few similar exact solutions [11, chs. IV and VI]. In particular, the simplest version of all variants analysed there, lead to an analytical solution at least so complex as that of the M/M/1 queue [11, pp. 67 and 70].

To compute the solution with accuracy one must deduce suitable homogeneous recurrence relations of a part of it, containing, at least, the infinite sum of terms with the Bessel functions. This has been in fact the case for the aforesaid simplest version of the biofilm model. A suitable adaptation of the already known three terms recurrence (TTR) Miller algorithm [12] for the functions $J_n(x)$ and $I_n(x)$ to this new context in which recurrences have now more than tree terms has been done.

Miller applied backward recurrence "for evaluating sequences of functions { f_k} when the recurrence connecting successive members was unstable for increasing k" as published Thacher [13]. Applying an algorithm like Miller´s (TTR) [12], we performed an exact calculation and graphic representation of such kind of solutions, with a five term recurrence, also applied in backwards calculation. Consequently we have applyed, in the simplest version of our biofilm model, a generalization of that algorithm including the whole infinite sum in functions { f_k} and not only one Bessel function. So the recurrences obtained have more than tree terms, as expected according to the additional complexity of the functions.

The early stages of growth and accumulation of biofilm included in that model, was the subject of [11] jointly with the search of how to deal when facing theoretical models near the border of mathematic intractability. Accordingly, those early stages can be modeled by several more complicated versions than the one deduced in this work, which is only a first approach.

Besides this first version wich we call "Mono-layered concentrated growth" kinetics, we, also, for sake of completeness, described in [11] how to reach solutions for three more approaches: Zero order kinetics, "Blackman inspired" kinetics and "Averaged" first order kinetics, all known in biotechnological literature. Those approaches are, however, only particular cases of the main task, which is the mathematical deduction of the exact solution for Monod kinetic law. We have already reach such general version of the model [11, Chap. VI].

As conclusion a Bessel functions framework seems to be appropriate for modeling biofilm formation and growth dynamics. The ideas and the model described here are only the beginning of the modeling possibilities offered by that mathematic framework.

In Queuing Theory utilization of State-Transition-Rate Diagrams is a customary tool for description of a particular queue dynamics under analysis. We also constructed the equivalent diagram for biofilm model, lightning this way an "isomorphism" between the two contexts [11, p. 182]. Accordingly with this circumstance, a careful analysis of Clarke classical solution [14] and our previous work [11] allows to put in equation and reach the transient solution of many more queues [11, Chap. VII, pp. 167-180]. Such unifying

way will allow, with a unique methodology, obtain exactly solutions in many models. Transient phases in Queuing Theory is a subject that we will leave for future work.

2. Skope and structure of this work

The biofilm theoretical model is briefly described in Part I. The mathematical resolution is accomplished in Part II, the deduction of an algorithm similar to Miller´s three term recurrence is deduced in Part III and some numerical simulations are presented in Part IV. Conclusions and future work are in Part V.

Part I

3. Theoretical model brief description

A brief description of the model can be made with figures 1, 2 and 3. The model postulates a layered structure to describe that the thickness of the biofilm is not uniform as in Fig. 1.
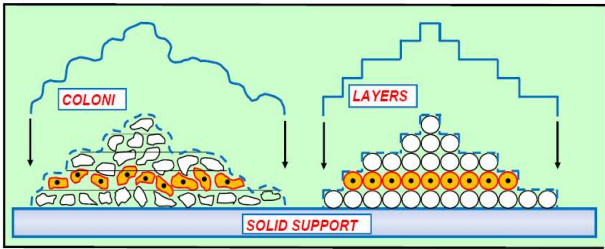

Fig. 1. The biofilm space is divided by layers each of them

with height equal to the mean linear bacteria dimension,

including the surrounding extracellular polymer.

The kinetics of biofilm formation and growth , over time, is obtained computing the S_n areas defined in Fig. 2 as functions of time.
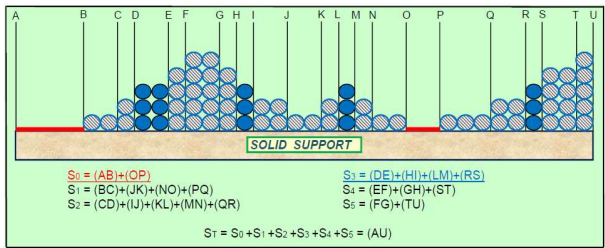

Fig. 2. This diagram illustrate and explains the quantitative

segmentation of the solid support total area (S_T) referred in the text.

It is also considered a gradient of nutrient concentration, from the outermost layer into the biofilm, along L layers. The nutrient concentration profile is postulated to decreases linearly, from layer to layer, from the outside to the inside, until it reaches zero after (L + 1) layers. This linearization is only a first approach in the context of this most simple version of the model. In Fig. 3, it is L = 4.
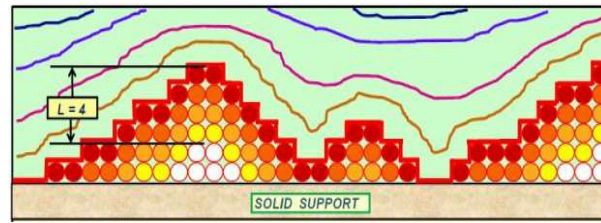
Fig. 3. This diagram illustrate the two populations of bacteria:
active (colored from red to yellow) and inactive (in white).
In active population red means the highest concentration of
substrate, yellow the lowest one and in inactive population
white means that there is no substrate

In areas S_n where $n > L$, all the layers below the first L from above are inactive and do not consume nutrients. The bacteria in the layers in which exists nutrient are active and can reproduce, thus contributing to the increase in biomass. The nutrient concentration in each layer determines the specific growth rates of bacteria in that layer.

The partial processes that contribute to the formation and growth of biofilm are:

1 - The adhesion of planktonic bacteria to the solid support or to other bacteria already adhered. To quantify this process, a flow F is defined as the area covered by the bacteria that adhere, per area of the solid support and time unit.

2 - The desorption of the adhered bacteria, defining, for the top layer of each S_n a kinetic constant k_n. This constant is defined as the vacant area left by bacteria that desorbs, per area S_n and time unit.

3 - The specific growth rates of bacteria in the active layers, quantified by $\mu_j = \mu_{máx.} \cdot \eta_j(C_j)$ in which $\mu_{máx.}$ is the maximum specific growth rate and η_j is the remaining factor that depends on the nutrient concentration at the considered layer.

4 - The maximum specific growth rates are decomposed in the directions parallel and perpendicular to the solid support thus getting defined two specific growth rates: $\vec{\mu_j} = \vec{\mu_{máx.}} \cdot \eta_j(C_j)$ and $\mu_j^{\uparrow} = \mu_{máx.}^{\uparrow} \cdot \eta_j(C_j)$

More minor details can be found in [11, Chaps. I, II, III]. Accounting for all these partial processes we obtain a system of differential-difference master equations whose solution will be the functions $S_n = S_n(t)$ for $n \geq 0$.

Part II
Theoretical model resolution

4. Governing equation system definition

We start the resolution of our model writing the total system of differential-difference master equations obtained in [11, Chap. III, Box 5].

The system reads, from (1) to (4):

$$\left(\frac{dS_0}{dt} \right) = -\boldsymbol{F} \cdot S_0 + \left(k_1 - \vec{\mu_{máx.}} \cdot \eta_1 \right) \cdot S_1 - \vec{\mu_{máx.}} \cdot \left(\sum_{j=2}^{L} \eta_j \cdot S_j \right) \tag{1}$$

$$\left(\frac{dS_1}{dt}\right) = \boldsymbol{F} \cdot S_0 + \left[\left(\mu^{\rightarrow}_{m\acute{a}x.} - \mu^{\uparrow}_{m\acute{a}x.}\right) \cdot \eta_1 - \boldsymbol{F} - k_1\right] \cdot S_1 + \left[k_2 + \mu^{\rightarrow}_{m\acute{a}x.} \cdot \left(\eta_2 - \eta_1\right)\right] \cdot S_2 +$$

$$+ \mu^{\rightarrow}_{m\acute{a}x.} \cdot \left[\sum_{j=3}^{L} (\eta_j - \eta_{j-1}) \cdot S_j\right] - \mu^{\rightarrow}_{m\acute{a}x.} \cdot \eta_L \cdot S_{L+1} \qquad (2)$$

$$\left(\frac{dS_n}{dt}\right) = \left[\boldsymbol{F} + \mu^{\uparrow}_{m\acute{a}x.} \cdot \left(\sum_{j=1}^{n-1} \eta_j\right)\right] \cdot S_{n-1} + \left[-\boldsymbol{F} + \mu^{\rightarrow}_{m\acute{a}x.} \cdot \eta_1 - \mu^{\uparrow}_{m\acute{a}x.} \cdot \left(\sum_{j=1}^{n} \eta_j\right) - k_n\right] \cdot S_n +$$

$$+ \left[\mu^{\rightarrow}_{m\acute{a}x.} \cdot (\eta_2 - \eta_1) + k_{n+1}\right] \cdot S_{n+1} + \mu^{\rightarrow}_{m\acute{a}x.} \cdot \left[\sum_{j=2}^{L-1} (\eta_{j+1} - \eta_j) \cdot S_{n+j}\right] - \mu^{\rightarrow}_{m\acute{a}x.} \cdot \eta_L \cdot S_{n+L}$$

$$\ldots \text{ if } (2 \leq n \leq L) \qquad (3)$$

$$\left(\frac{dS_n}{dt}\right) = \left[\boldsymbol{F} + \mu^{\uparrow}_{m\acute{a}x.} \cdot \left(\sum_{j=1}^{L} \eta_j\right)\right] \cdot S_{n-1} + \left[-\boldsymbol{F} + \mu^{\rightarrow}_{m\acute{a}x.} \cdot \eta_1 - \mu^{\uparrow}_{m\acute{a}x.} \cdot \left(\sum_{j=1}^{L} \eta_j\right) - k_n\right] \cdot S_n +$$

$$+ \left[\mu^{\rightarrow}_{m\acute{a}x.} \cdot (\eta_2 - \eta_1) + k_{n+1}\right] \cdot S_{n+1} + \mu^{\rightarrow}_{m\acute{a}x.} \cdot \left[\sum_{j=2}^{L-1} (\eta_{j+1} - \eta_j) \cdot S_{n+j}\right] - \mu^{\rightarrow}_{m\acute{a}x.} \cdot \eta_L \cdot S_{n+L}$$

$$\ldots \text{ if } (n>L) \qquad (4)$$

And we recall the notation defined in [11, Chap. II, pp. 11 to 19]

S_n - area covered with n layers

S_T - solid flat carrier total area

L - maximum number of active layers in each area S_n . If n<L all the layers are active, if n>L only L layers are active, and (n-L) inactive.

t - time

$\boldsymbol{F}$ - attachment flux of planktonic bacteria expressed in flat area covered per total carrier area S_T and time unit

k_n - kinetic constant for the process of biomass desorption (or detachment)

$\mu^{\rightarrow}_{m\acute{a}x.}$ - maximum specific growth rate in the direction parallel to the solid support

$\mu^{\uparrow}_{m\acute{a}x.}$ - maximum specific growth rate in the direction perpendicular to the solid support

η_j - remaining factor, besides the maximums specific growth rates, in the Monod specific growth rate model. See [11, Chap. III, pp. 25].

j -number, from 1 to L, and from top outermost layer to down innermost still active layer in any area S_n [11, Chap. III, pp. 25].

This system accounts the variation with time of all S_n (n = 0, 1, 2, …, n, …).

All terms with common S_n are colected together and are disposed in increased order (n) in the right hand sides. We observe that the system structure consists in,

$\left(\dfrac{dS_0}{dt}\right)$: one differential equation

$\left(\dfrac{dS_1}{dt}\right)$: one differential equation

$\left(\dfrac{dS_n}{dt}\right)$ if $(2 \le n \le L)$: $(L-1)$ differential equations

$\left(\dfrac{dS_n}{dt}\right)$ if $(n>L)$: infinite number of differential equations

The dimensionless variables and parameters that we choose are defined from (5) to (11):

$$\tau = \left(\mu_{máx.}^{\rightarrow} + \mu_{máx.}^{\uparrow}\right) \cdot \eta_1 \cdot t \tag{5}$$

$$\theta_n = \frac{S_n}{S_T} \tag{6}$$

$$\rho = \frac{F}{\left(\mu_{máx.}^{\rightarrow} + \mu_{máx.}^{\uparrow}\right) \cdot \eta_1} \tag{7}$$

$$\Phi = \frac{\mu_{máx.}^{\uparrow}}{\left(\mu_{máx.}^{\rightarrow} + \mu_{máx.}^{\uparrow}\right)} \tag{8}$$

$$(1 - \Phi) = \frac{\mu_{máx.}^{\rightarrow}}{\left(\mu_{máx.}^{\rightarrow} + \mu_{máx.}^{\uparrow}\right)} \tag{9}$$

$$\delta_n = \frac{k_n}{\left(\mu_{máx.}^{\rightarrow} + \mu_{máx.}^{\uparrow}\right) \cdot \eta_1} \tag{10}$$

$$\psi_j = \frac{\eta_j}{\eta_1} \tag{11}$$

Before insert the dimensionless parameters it is convenient put in evidence the kinetic factor η_1 whenever it occurs to facilitate the substitution of ψ_j. This is done from (12) to (15).

$$\left(\frac{dS_0}{dt}\right) = -\boldsymbol{F} \cdot S_0 + \left(k_1 - \mu_{máx.}^{\rightarrow} \cdot \eta_1\right) \cdot S_1 - \mu_{máx.}^{\rightarrow} \cdot \eta_1 \cdot \left[\sum_{j=2}^{L} \left(\frac{\eta_j}{\eta_1}\right) \cdot S_j\right] \tag{12}$$

$$\left(\frac{dS_1}{dt}\right) = \boldsymbol{F} \cdot S_0 + \left[\left(\mu_{máx.}^{\rightarrow} - \mu_{máx.}^{\uparrow}\right) \cdot \eta_1 - \boldsymbol{F} - k_1\right] \cdot S_1 + \left[k_2 + \mu_{máx.}^{\rightarrow} \cdot \eta_1 \cdot \left(\frac{\eta_2}{\eta_1} - 1\right)\right] \cdot S_2 +$$

$$+ \mu_{máx.}^{\rightarrow} \cdot \eta_1 \cdot \left[\sum_{j=3}^{L} \left(\frac{\eta_j}{\eta_1} - \frac{\eta_{j-1}}{\eta_1}\right) \cdot S_j\right] - \mu_{máx.}^{\rightarrow} \cdot \eta_1 \cdot \left(\frac{\eta_L}{\eta_1}\right) \cdot S_{L+1} \tag{13}$$

$$\left(\frac{dS_n}{dt}\right) = \left\{\boldsymbol{F} + \mu_{máx.}^{\uparrow} \cdot \eta_1 \cdot \left[\sum_{j=1}^{n-1} \left(\frac{\eta_j}{\eta_1}\right)\right]\right\} \cdot S_{n-1} - \left\{\boldsymbol{F} - \mu_{máx.}^{\rightarrow} \cdot \eta_1 + \mu_{máx.}^{\uparrow} \cdot \eta_1 \cdot \left[\sum_{j=1}^{n} \left(\frac{\eta_j}{\eta_1}\right)\right] + k_n\right\} \cdot S_n +$$

$$+ \left[\mu_{máx.}^{\rightarrow} \cdot \eta_1 \cdot \left(\frac{\eta_2}{\eta_1} - 1\right) + k_{n+1}\right] \cdot S_{n+1} + \mu_{máx.}^{\rightarrow} \cdot \eta_1 \cdot \left[\sum_{j=2}^{L-1} \left(\frac{\eta_{j+1}}{\eta_1} - \frac{\eta_j}{\eta_1}\right) \cdot S_{n+j}\right] - \mu_{máx.}^{\rightarrow} \cdot \eta_1 \cdot \left(\frac{\eta_L}{\eta_1}\right) \cdot S_{n+L}$$

$$\ldots \text{ if } (2 \le n \le L) \tag{14}$$

$$\left(\frac{dS_n}{dt}\right) = \left\{ F + \mu_{máx.}^{\uparrow} \cdot \eta_1 \cdot \left[\sum_{j=1}^{L} \left(\frac{\eta_j}{\eta_1}\right) \right] \right\} \cdot S_{n-1} - \left\{ F - \mu_{máx.}^{\rightarrow} \cdot \eta_1 + \mu_{máx.}^{\uparrow} \cdot \eta_1 \cdot \left[\sum_{j=1}^{L} \left(\frac{\eta_j}{\eta_1}\right) \right] + k_n \right\} \cdot S_n +$$

$$+ \left[\mu_{máx.}^{\rightarrow} \cdot \eta_1 \cdot \left(\frac{\eta_2}{\eta_1} - 1\right) + k_{n+1} \right] \cdot S_{n+1} + \mu_{máx.}^{\rightarrow} \cdot \eta_1 \cdot \left[\sum_{j=2}^{L-1} \left(\frac{\eta_{j+1}}{\eta_1} - \frac{\eta_j}{\eta_1}\right) \cdot S_{n+j} \right] - \mu_{máx.}^{\rightarrow} \cdot \eta_1 \cdot \left(\frac{\eta_L}{\eta_1}\right) \cdot S_{n+L}$$

$$\dots \text{ if } (n>L) \tag{15}$$

As consequence of (5) and (6) the derivatives $\left(\frac{dS_n}{dt}\right)$ on the left hand sides assume the form:

$$\left(\frac{dS_n}{dt}\right) = \frac{d(\theta_n \cdot S_T)}{d\left[\dfrac{\tau}{\eta_1\left(\mu_{máx.}^{\rightarrow} + \mu_{máx.}^{\uparrow}\right)}\right]} = \left(\mu_{máx.}^{\rightarrow} + \mu_{máx.}^{\uparrow}\right) \cdot \eta_1 \cdot S_T \cdot \left(\frac{d\theta_n}{d\tau}\right) \tag{16}$$

The next step is to divide all the equations by $\left[\left(\mu_{máx.}^{\rightarrow} + \mu_{máx.}^{\uparrow}\right) \cdot \eta_1 \cdot S_T\right]$ and we get immediately the dimensionless system, equations (17) to (20). Besides, initial condition (21) is part of the system, consequently also must be included.

$$\left(\frac{d\theta_0}{d\tau}\right) = -\rho \cdot \theta_0 + [\delta_1 - (1 - \Phi)] \cdot \theta_1 - (1 - \Phi) \cdot \left(\sum_{j=2}^{L} \psi_j \cdot \theta_j\right) \tag{17}$$

$$\left(\frac{d\theta_1}{d\tau}\right) = \rho \cdot \theta_0 + [(1 - 2 \cdot \Phi) - \rho - \delta_1] \cdot \theta_1 + [\delta_2 + (1 - \Phi) \cdot (\psi_2 - 1)] \cdot \theta_2 +$$

$$+ (1 - \Phi) \cdot \left[\sum_{j=3}^{L} (\psi_j - \psi_{j-1}) \cdot \theta_j \right] - (1 - \Phi) \cdot \psi_L \cdot \theta_{L+1} \tag{18}$$

$$\left(\frac{d\theta_n}{d\tau}\right) = \left[\rho + \Phi \cdot \left(\sum_{j=1}^{n-1} \psi_j \right) \right] \cdot \theta_{n-1} + \left[(1 - \Phi) - \rho - \Phi \cdot \left(\sum_{j=1}^{n} \psi_j \right) - \delta_n \right] \cdot \theta_n +$$

$$+ [(1 - \Phi) \cdot (\psi_2 - 1) + \delta_{n+1}] \cdot \theta_{n+1} + (1 - \Phi) \cdot \left[\sum_{j=2}^{L-1} (\psi_{j+1} - \psi_j) \cdot \theta_{n+j} \right] - (1 - \Phi) \cdot \psi_L \cdot \theta_{n+L}$$

$$\dots \text{ if } (2 \leq n \leq L) \tag{19}$$

$$\left(\frac{d\theta_n}{d\tau}\right) = \left[\rho + \Phi \cdot \left(\sum_{j=1}^{L} \psi_j \right) \right] \cdot \theta_{n-1} + \left[(1 - \Phi) - \rho - \Phi \cdot \left(\sum_{j=1}^{L} \psi_j \right) - \delta_n \right] \cdot \theta_n +$$

$$+ [(1 - \Phi) \cdot (\psi_2 - 1) + \delta_{n+1}] \cdot \theta_{n+1} + (1 - \Phi) \cdot \left[\sum_{j=2}^{L-1} (\psi_{j+1} - \psi_j) \cdot \theta_{n+j} \right] - (1 - \Phi) \cdot \psi_L \cdot \theta_{n+L}$$

$$\dots \text{ if } (n>L) \tag{20}$$

The initial condition must, of course, be:

$$\theta_0(0) = 1, \text{ and } \theta_n(0) = 0 \;\; for \; n>0 \tag{21}$$

(at the beginning (τ=0) al the solid support is bare)

5. General model resolution strategy: concept of "Mathematical meeting point"

This system of equations is composed by the so-called differential-difference equations. It is a traditionally difficult domain and suitable theory for this subject can be found in Pinney [15], Bellman and Cooke [16] and El´sgol´ts and Norkin [17] and certainly other more recent works.

Also formally similar problems arise in Operational Research literature, in particular when transient states are analysed in Queuing Theory.

In the present case the system has an analytical solution. However that solution can´t be represented, for the most general version, by a closed form, like a final expression $\theta_n = \theta_n(\tau)$, and we will only solve the model for a simplified case and extract observations from that resolution. Such observations will later allow to establish the method for more general cases.

A formalism similar to that of Clarke ([14], [18]) will be our working tool. Suitable modifications will be introduced to adapt such solving way to the particular details of our case. Clarke formalism can also be found described in Saaty [19] and Srivastava and Kashyap [20].

We will use the following strategy, in two steps, being only the first one the scope of this work. The second one will be next future work:

<u>First step</u>: We must solve the system for $L = 1$ and $\delta_1 = \delta_2 = \cdots = \delta_n = \cdots = \delta$. That is, for the case where there is only one active layer and erosion is of equal intensity in all the surface fractions θ_n $(n \geq 1)$. This one will be named the simplified version of the model. More specifically we can name this version the "Mono layered concentrated" growth kinetics variant, already defined in [11, Chap. III].

<u>Second step</u>: analyse the solution obtained in the first step, inspect their mathematical structure, and construct a suitable Guess Solution that will reduce all the solution of the complete system to an algebraic problem. The algebraic problem defined in this second step falls in the context of algebraic difference equations and is somewhat cumbersome. However it will be demonstrated that the complete resolution is possible. The aforesaid Guess Solution contains an infinite series of Bessel functions, each one multiplied by a respective labelled factor. All those factors must then be analytically determined on a recurring suitable scheme.

The system of the simplified "Mono layered concentrated" growth kinetics version, corresponding to the first step, is easily obtained from (17) to (21) inserting the conditions:

$$\delta_1 = \delta_2 = \cdots = \delta_n = \cdots = \delta \tag{22}$$

... and,

$$\psi_j = 0 \, , \ldots \ldots \ldots \; for \; j > 1 \; \ldots \ldots \ldots \, leaving \; L \geq 2 \tag{23}$$

Condition (23) is equivalent to impose $L = 1$ because all kinetic parameters ψ_j are annulled for $j \geq 2$. We also observe that (23) implicates the sameness between (18) and (19).

Consequently, the system for the simplified version is:

$$\left(\frac{d\theta_0}{d\tau}\right) = -\rho \cdot \theta_0 + [\delta - (1 - \varPhi)] \cdot \theta_1 \tag{24}$$

$$\left(\frac{d\theta_1}{d\tau}\right) = \rho \cdot \theta_0 + [(1 - 2 \cdot \varPhi) - \rho - \delta] \cdot \theta_1 + [\delta - (1 - \varPhi)] \cdot \theta_2 \tag{25}$$

$$\left(\frac{d\theta_n}{d\tau}\right) = (\rho + \varPhi) \cdot \theta_{n-1} + [(1 - \varPhi) - \rho - \varPhi - \delta] \cdot \theta_n + [\delta - (1 - \varPhi)] \cdot \theta_{n+1}$$

$$\text{... if } (n \geq 2) \tag{26}$$

With initial condition:

$$\theta_0(0) = 1, \quad \text{and} \quad \theta_n(0) = 0 \qquad\qquad for \; n>0 \tag{27}$$

We have already defined, as work context, [[11, p. 19, figs. 6 to 11] the five specific growth rate kinetics:
- Monod kinetics
- Zero order kinetics
- "Blackman inspired" kinetics
- "Averaged" first order kinetics
- "Mono-layered concentrated growth" kinetics

When $L = 1$ the first four (Monod, Zero order, "Blackman inspired" and "Averaged" first order) reduce in complexity and becomes equal to "Mono-layered concentrated growth" kinetics model. So we can conclude that to solve this last model is equivalent to solve the most simplified version of all the other four. We can consider "Mono-layered concentrated growth" kinetics as a sort of "mathematical meeting point" of all the kinetics under our analysis.

6. "Mono layered concentrated" growth kinetics: exact solution

6.1 Common initial steps: generating function formalism

The first step to start the resolution is to make the substitution,

$$\theta_n(\tau) = e^{-(\rho+2\cdot\Phi-\delta-1)\cdot\tau} \cdot Q_n(\tau) \tag{28}$$

This substitution aims to simplify the system by eliminating the term relative to index (n) on the right hand side, in all the equations for $(n \geq 1)$. After simplification we get, from (29) to (31),

$$\left(\frac{dQ_0}{d\tau}\right) = (2\cdot\Phi+\delta-1)\cdot Q_0 - (1-\Phi-\delta)\cdot Q_1 \tag{29}$$

$$\left(\frac{dQ_1}{d\tau}\right) = \rho \cdot Q_0 - (1-\Phi-\delta)\cdot Q_2 \tag{30}$$

$$\left(\frac{dQ_n}{d\tau}\right) = (\rho+\Phi)\cdot Q_{n-1} - (1-\Phi-\delta)\cdot Q_{n+1}$$

$$\dots \; if \; (n \geq 2) \tag{31}$$

With initial condition:

$$Q_0(0) = 1, \quad and \quad Q_n(0) = 0 \; for \; n>0 \tag{32}$$

Let now define the following generating function,

$$G(z,\tau) = \sum_{n=0}^{\infty} a_n \cdot Q_n(\tau) \cdot \frac{(\tau-z)^n}{n!} \tag{33}$$

... similar to that one of Clarke ([14], [18]),

$$G(z,\tau) = \sum_{n=0}^{\infty} Q_n(\tau) \cdot \frac{(z-\tau)^n}{n!} \tag{34}$$

... but with additional coefficients a_n which remain to be determined and with changed signs at τ and z. These modifications are justified because the system solved by Clarke is,

$$\left(\frac{dQ_0}{d\tau}\right) = Q_0 + Q_1 \tag{35}$$

$$\left(\frac{dQ_n}{d\tau}\right) = \rho \cdot Q_{n-1} + Q_n \qquad \dots if \; (n \geq 1) \tag{36}$$

Therefore this is a simpler system because Φ and δ are null which is not the case of our system. This explains the need to include the coefficients a_n . Another difference lies in the exchanged signs in the functions $Q_n(\tau)$ which explains the need to change the signs in τ and z in the generating function. Like in Clarke ([14], [18]) here we also seek for a generating function, $G(z,\tau)$ such that obeys a differential equation like,

$$\frac{\partial^2 G(z,\tau)}{\partial\tau\,\partial z} = Constant \cdot G(z,\tau) \tag{37}$$

Which is the so called Telegraph equation. The suitable deduction of coefficients a_n will accomplish that goal.

First, $\dfrac{\partial^2 G(z,\tau)}{\partial\tau\,\partial z}$ must be obtained from (33). We get,

$$\frac{\partial^2 G(z,\tau)}{\partial\tau\,\partial z} = -a_1 \cdot \frac{dQ_1}{d\tau} - \sum_{n=2}^{\infty} a_n \cdot \frac{dQ_n}{d\tau} \cdot \frac{(\tau-z)^{n-1}}{(n-1)!} - \sum_{n=2}^{\infty} a_n \cdot Q_n \cdot \frac{(\tau-z)^{n-2}}{(n-2)!} \tag{38}$$

The order of partial derivations is indifferent,

$$\frac{\partial^2 G(z,\tau)}{\partial\tau\,\partial z} = \frac{\partial^2 G(z,\tau)}{\partial z\partial\tau} \tag{39}$$

Now, taking the expressions for $\frac{dQ_n}{d\tau}$ with $n \geq 1$ given by (30) and (31) we get,

$$\frac{\partial^2 G(z,\tau)}{\partial\tau\,\partial z} = -a_1 \cdot \rho \cdot Q_0 - (\rho+\Phi) \cdot \sum_{n=2}^{\infty} a_n \cdot Q_{n-1} \cdot \frac{(\tau-z)^{n-1}}{(n-1)!} -$$
$$- \sum_{n=2}^{\infty} [a_{n-1} \cdot (1-\Phi-\delta) - a_n] \cdot Q_n \cdot \frac{(\tau-z)^{n-2}}{(n-2)!} \tag{40}$$

The usefulness of coefficients a_n is now proved inspecting the second summation because we want to cancel it. The reason is that the exponents in $(\tau-z)$ is two units lower than the corresponding order of functions Q_n and this summation cancelation would not be possible if all coefficients a_n where equal to 1, like in Clarke´s generating function. Determination of coefficients a_n is easy and follows straightaway.

Must be,

$$a_{n-1} \cdot (1-\Phi-\delta) - a_n = 0 \quad \dots for\ (n \geq 2) \tag{41}$$

We get immediately the solution,

$$a_n = a_1 \cdot (1-\Phi-\delta)^{n-1} \quad \dots for\ (n \geq 2) \tag{42}$$

Substituting (42) in (40) the Telegraph equation now reads,

$$\frac{\partial^2 G(z,\tau)}{\partial\tau\,\partial z} =$$
$$= -(\rho+\Phi) \cdot (1-\Phi-\delta) \cdot \left[a_1 \cdot \frac{\rho}{(\rho+\Phi) \cdot (1-\Phi-\delta)} \cdot Q_0 + a_1 \cdot \sum_{n=1}^{\infty} (1-\Phi-\delta)^{n-1} \cdot Q_n \cdot \frac{(\tau-z)^n}{(n)!} \right] \tag{43}$$

Putting,

$$a_0 = a_1 \cdot \frac{\rho}{(\rho+\Phi) \cdot (1-\Phi-\delta)} \tag{44}$$

… equation (43) becomes,

$$\frac{\partial^2 G(z,\tau)}{\partial\tau\,\partial z} = -(\rho+\Phi) \cdot (1-\Phi-\delta) \cdot \sum_{n=0}^{\infty} a_n \cdot Q_n \cdot \frac{(\tau-z)^n}{(n)!} \tag{45}$$

This right hand side is equal to $G(z,\tau)$ multiplied by $[-(\rho+\Phi) \cdot (1-\Phi-\delta)]$, which is constant. As proposed, a Telegraph equation is now reached. The coefficient a_0 can be equal to 1 for the sake of simplification. Consequently all the a_n are now defined,

$$a_0 = 1 \tag{46}$$

… and
$$a_n = \frac{(\rho+\Phi)}{\rho} \cdot (1-\Phi-\delta)^n \quad \dots for\ (n \geq$$

1) $\qquad\qquad$ (47)

Till now holds,

$$\frac{\partial^2 G(z,\tau)}{\partial\tau\,\partial z} = -(\rho+\Phi) \cdot (1-\Phi-\delta) \cdot G(z,\tau) \quad \text{(Telegraph equation)} \tag{48}$$

... where,

$$G(z,\tau) = Q_0(\tau) + \frac{(\rho + \Phi)}{\rho} \cdot \sum_{n=1}^{\infty} (1 - \Phi - \delta)^n \cdot Q_n(\tau) \cdot \frac{(z - \tau)^n}{n!} \tag{49}$$

Now equation (29) and condition (32) will come into play. According to (32), at time $(\tau = 0)$, the generating function must be $G(z,\tau) = Q_0(0) = 1$. So, condition (32) now reads. in generating function formalism,

$$G(z,0) = 1 \tag{50}$$

With (49) the partial derivative $\left(\dfrac{\partial G}{\partial \tau}\right)$ can be easily obtained,

$$\left(\frac{\partial G}{\partial \tau}\right) = \frac{dQ_0}{d\tau} + \frac{(\rho + \Phi)}{\rho} \cdot \sum_{n=1}^{\infty} (1 - \Phi - \delta)^n \cdot \frac{dQ_n}{d\tau} \cdot \frac{(\tau - z)^n}{n!} +$$

$$+ \frac{(\rho + \Phi)}{\rho} \cdot \sum_{n=1}^{\infty} (1 - \Phi - \delta)^n \cdot Q_n \cdot \frac{(\tau - z)^{n-1}}{(n - 1)!} \tag{51}$$

When $(z = \tau)$,

$$\left(\frac{\partial G}{\partial \tau}\right)_{z=\tau} = \frac{dQ_0}{d\tau} + \frac{(\rho + \Phi)}{\rho} \cdot (1 - \Phi - \delta) \cdot Q_1 \tag{52}$$

Inserting here equation (29) one gets,

$$\left(\frac{\partial G}{\partial \tau}\right)_{z=\tau} = (2 \cdot \Phi + \delta - 1) \cdot Q_0 + \frac{(1 - \Phi - \delta) \cdot \Phi}{\rho} \cdot Q_1 \tag{53}$$

But,

$$Q_0(\tau) = G(\tau, \tau) \tag{54}$$

... and,

$$\frac{\partial G}{\partial z} = -\frac{(\rho + \Phi)}{\rho} \cdot \sum_{n=1}^{\infty} (1 - \Phi - \delta)^n \cdot Q_n(\tau) \cdot \frac{(\tau - z)^{n-1}}{(n - 1)!} \tag{55}$$

What means,

$$\left(\frac{\partial G}{\partial z}\right)_{z=\tau} = -\frac{(\rho + \Phi)}{\rho} \cdot (1 - \Phi - \delta) \cdot Q_1(\tau) \tag{56}$$

.. and, consequently,

$$Q_1(\tau) = -\frac{\rho}{(\rho + \Phi) \cdot (1 - \Phi - \delta)} \cdot \left(\frac{\partial G}{\partial z}\right)_{z=\tau} \tag{57}$$

Equations (54) and (57) are now included in (53) and, in this way, the last condition for complete definition of the problem, in generating function context, is,

$$\left(\frac{\partial G}{\partial \tau}\right)_{z=\tau} = (2 \cdot \Phi + \delta - 1) \cdot G(\tau, \tau) - \frac{\Phi}{(\rho + \Phi)} \cdot \left(\frac{\partial G}{\partial z}\right)_{z=\tau} \tag{58}$$

Once deduced, the generating function $G(z,\tau)$ will conduct easily to all the functions $Q_n(\tau)$.
In fact from (49) one can conclude that,

$$Q_0(\tau) = G(\tau, \tau) \qquad (\textit{already obtained before}) \tag{59}$$

... and,

$$Q_n(\tau) = -\frac{(-1)^n \cdot \rho}{(\rho + \Phi) \cdot (1 - \Phi - \delta)^n} \cdot \left(\frac{\partial^n G}{\partial z^n}\right)_{z=\tau} \quad \ldots \ldots for \ (n \geq 1) \tag{60}$$

This last formula is easy to demonstrate, so we omit the details. Lastly, with (28), fractions $\theta_n(\tau)$ are calculated from the functions $Q_n(\tau)$. Then we will reach the solution of the simplified version of the model which

is also the "mathematical meeting point" for all the kinetic variants under analysis. A summary of what has been obtained so far in this generating function formalism, and will be used in the sequel, is, from (I) to (VII),

$I)$ $\left(\dfrac{\partial^2 G}{\partial z\,\partial \tau}\right) = -(\rho + \Phi)\cdot(1 - \Phi - \delta)\cdot G(z,\tau)$

(Telegraph equation)   (48)

$II)$ $G(z,0) = 1$ (Initial time condition)   (50)

$III)$ $\left(\dfrac{\partial G}{\partial \tau}\right)_{z=\tau} = (2\cdot \Phi + \delta - 1)\cdot G(\tau,\tau) -$

$\qquad\qquad\qquad -\dfrac{\Phi}{(\rho+\Phi)}\cdot\left(\dfrac{\partial G}{\partial z}\right)_{z=\tau}$ (First equation border condition)   (58)

$IV)$ $G(z,\tau) = Q_0(\tau) + \dfrac{(\rho+\Phi)}{\rho}\cdot\displaystyle\sum_{n=1}^{\infty}(1-\Phi-\delta)^n\cdot Q_n(\tau)\cdot\dfrac{(z-\tau)^n}{n!}$

(Generating function)   (49)

$V)$ $Q_0(\tau) = G(\tau,\tau)$ (Obtaining Q_0)   (59)

$VI)$ $Q_n(\tau) = -\dfrac{(-1)^n\cdot\rho}{(\rho+\Phi)\cdot(1-\Phi-\delta)^n}\cdot\left(\dfrac{\partial^n G}{\partial z^n}\right)_{z=\tau}\;\dots\dots for\;(n\geq 1)$

(Obtaining Q_n for $n\geq 1$)   (60)

$VII)$ $\theta_n(\tau) = e^{-(\rho+2\cdot\Phi-\delta-1)\cdot\tau}\cdot Q_n(\tau)$

(Obtaining θ_n from Q_n)   (28)

Telegraph equation (48) is solved applying Laplace transform over variable z. Applying first to the left hand side, one gets,

$\mathcal{L}\left\{\dfrac{\partial}{\partial z}\cdot\left[\dfrac{\partial G}{\partial \tau}\right]\right\} = \displaystyle\int_0^\infty e^{-s\cdot z}\cdot\dfrac{\partial}{\partial z}\cdot\left[\dfrac{\partial G}{\partial \tau}\right]\cdot dz$

(definition of Laplace transform)   (61)

$\displaystyle\int_0^\infty e^{-s\cdot z}\cdot\dfrac{\partial}{\partial z}\cdot\left[\dfrac{\partial G}{\partial \tau}\right]\cdot dz = s\cdot\mathcal{L}\left[\dfrac{\partial G}{\partial \tau}\right] - \left(\dfrac{\partial G}{\partial \tau}\right)_{z=0} = s\cdot\dfrac{\partial g(s,\tau)}{\partial \tau} - f(\tau)$ (62)

The function $g(s,\tau)$ is the Laplace transform of $G(z,\tau)$ and,

$$f(\tau) = \left[\dfrac{\partial G(z,\tau)}{\partial \tau}\right]_{z=0}$$ (63)

Similarly, applying the transform to the right hand side,

$$\mathcal{L}[-(\rho + \Phi) \cdot (1 - \Phi - \delta) \cdot G(z, \tau)] = -(\rho + \Phi) \cdot (1 - \Phi - \delta) \cdot g(s, \tau) \tag{64}$$

The right had sides in (62) and (64) must be equal,

$$s \cdot \frac{\partial g(s, \tau)}{\partial \tau} - f(\tau) = -(\rho + \Phi) \cdot (1 - \Phi - \delta) \cdot g(s, \tau) \tag{65}$$

The initial time condition (50) after Laplace transform reads,

$$\mathcal{L}[G(z, 0)] = \mathcal{L}(1) \tag{66}$$

... which is equivalent to,

$$g(s, 0) = \frac{1}{s} \tag{67}$$

The general solution of (65) is known from mathematical tables,

$$g(s, \tau) = e^{-(\rho + \Phi) \cdot (1 - \Phi - \delta) \cdot \frac{\tau}{s}} \cdot \left[\frac{1}{s} \cdot \int f(\tau) \cdot e^{(\rho + \Phi) \cdot (1 - \Phi - \delta) \frac{\tau}{s}} \cdot d\tau + C(s) \right] \tag{68}$$

The integration "constant" $C(s)$ is only constant relatively to time τ and only depends on s.
Inserting condition (67) and making $\tau = 0$ one can get $C(s)$.
From (68),

$$g(s, 0) = \frac{1}{s} \cdot \left[\int f(\tau) \cdot e^{(\rho + \Phi) \cdot (1 - \Phi - \delta) \cdot \frac{\tau}{s}} \cdot d\tau \right]_{\tau = 0} + C(s) \tag{69}$$

Substitution of (67) here leads to,

$$C(s) = \frac{1}{s} \cdot \left\{ 1 - \left[\int f(\tau) \cdot e^{(\rho + \Phi) \cdot (1 - \Phi - \delta) \cdot \frac{\tau}{s}} \cdot d\tau \right]_{\tau = 0} \right\} \tag{70}$$

Now is easy to particularize the general solution (68) for our case, inserting there this expression of $C(s)$,

$$g(s, \tau) = \frac{e^{-(\rho + \Phi) \cdot (1 - \Phi - \delta) \frac{\tau}{s}}}{s} + \int_0^\tau f(\sigma) \cdot \frac{e^{-(\rho + \Phi) \cdot (1 - \Phi - \delta) \cdot \frac{(\tau - \sigma)}{s}}}{s} \cdot d\sigma \tag{71}$$

An observation must be made about the change of τ by σ as integration variable. This has been done with the purpose of avoid confusion between that variable and the superior limit in the integral.

6.2 Trifurcation stage: continuous biofilm, patchy biofilm and border case

In the sequel, application of inverse Laplace transform leads back again to the generating function $G(z, \tau)$. We must now consider tree hypotheses depending on the relative values of parameters δ and $(1 - \Phi)$. As bigger is δ, or as littler is $(1 - \Phi)$, more the process of erosion is important in their intensity, comparatively to the process of bacterial growth inside the biofilm. In mathematical context this is compulsory because if the sign in the exponentials is positive the inverse transform is one, if it is null is another and if it is negative is yet another one.
Explicitly,
Case 1) If $\delta < (1 - \Phi)$, the inverse transform reads,

$$\mathcal{L}^{-1} \left\{ \frac{e^{-a \cdot \frac{\tau}{s}}}{s} \right\} = J_0 \left(2 \cdot \sqrt{a \cdot \tau \cdot z} \right) \dots \dots where \ a = (\rho + \Phi) \cdot (1 - \Phi - \delta) > 0 \tag{72}$$

Case 2) If $\delta > (1 - \Phi)$, the inverse transform reads,

$$\mathcal{L}^{-1}\left\{\frac{e^{+a\cdot\frac{\tau}{s}}}{s}\right\} = I_0\left(2\cdot\sqrt{a\cdot\tau\cdot z}\right)\dots\dots where\ a = (\rho+\Phi)\cdot(\Phi+\delta-1) > 0 \tag{73}$$

Case 3) If $\delta = (1-\Phi)$, the inverse transform reads,

$$\mathcal{L}^{-1}\left\{\frac{1}{s}\right\} = 1\dots\dots in\ this\ borderline\ case,\ \ a = 0 \tag{74}$$

The functions in Cases 1 and 2 are respectively Bessel functions and Modified Bessel functions of first kind of order zero. Bessel function of first kind of order n is defined by,

$$J_n(x) = \sum_{k=0}^{\infty}\frac{(-1)^k(x/2)^{n+2k}}{k!\,\Gamma(n+k+1)} \tag{75}$$

... and Modified Bessel function of first kind of order n by,

$$I_n(x) = \sum_{k=0}^{\infty}\frac{\left(\frac{x}{2}\right)^{n+2k}}{k!\,\Gamma(n+k+1)} \tag{76}$$

Here $\Gamma(x)$ is the gamma function. When $x = 1, 2, 3, \dots$ then,

$$\Gamma(x) = (x-1)! \tag{77}$$

In our case $n = 0$, so $\Gamma(n+k+1) = \Gamma(k+1) = k!$ and we can write,

$$J_0(x) = \sum_{k=0}^{\infty}\frac{(-1)^k(x/2)^{2k}}{(k!)^2} \tag{78}$$

... and,

$$I_0(x) = \sum_{k=0}^{\infty}\frac{(x/2)^{2k}}{(k!)^2} \tag{79}$$

As indicated before, in the first stages of biofilm formation erosion is seldom the most intense process. In most of situations growth as consequence of active bacterial reproduction is nearly the only relevant process. This corresponds, in mathematical terms to the aforesaid Case 1. And we can classify the obtained biofilm as a "continuous biofilm".

However, patchy biofilms, also exists everywhere if erosion becomes strong enough in those initial times of development, leading to a steady state where bare areas of solid support exist in finite extension,   even after a long time, and biomass remains only accumulated   in colonies or clusters without a complete coverage of solid support area.

The designation "patchy biofilm" is opposed, or complementary to "continuous biofilm" in this physical classification. Consequently we observe that this mathematical formalism can translate this duality in biofilm structure, relating different biofilm morphologies with different mathematical functions. Such translation gets more visibility, principally when achieved formulas are graphically   represented. Case 3 is the border case and the limit value of the bare fraction, $\theta_0(\tau)$, is zero at infinite time τ, as expected.

Complete coverage of initial support bare area is rendered complete, after some time, in the case of con-tinuous biofilm. After that time τ, the fraction $\theta_0(\tau)$ assume negative values, and those values are not physically possible. Consequently one must initiate a new time interval calculation where $\theta_0(\tau)$ no longer

came into play and successively and so on, later, with $\theta_1(\tau), \theta_2(\tau)$ ... by the same reasons. But this is beyond the scope of the present work.

The analytical solutions for the aforesaid tree cases are,

Solution for Case 1: continuous biofilm: [δ<(1 − Φ)]

$$\theta_n(\tau) = \alpha_n \cdot e^y \cdot \sum_{k=0}^{\infty} \beta_k \cdot J_{n+k}(x) \tag{80}$$

Where:

$x = 2 \cdot \tau \cdot \sqrt{(\rho + \Phi) \cdot (1 - \Phi - \delta)}$

$y = (1 - \rho - 2 \cdot \Phi - \delta) \cdot \tau$

$\alpha_0 = 1$

$\alpha_n = \dfrac{\rho \cdot (\rho + \Phi)^{n-1}}{\sqrt{(\rho + \Phi)^n \cdot (1 - \Phi - \delta)^n}} \ \dots only\ for\ n \geq 1$

$\beta_0 = 1$

$\beta_1 = \dfrac{(2 \cdot \Phi + \delta - 1)}{\sqrt{(\rho + \Phi) \cdot (1 - \Phi - \delta)}}$

$\beta_k = \dfrac{\{[\rho \cdot (1 - \Phi - \delta) + \Phi \cdot (1 - \delta)] \cdot \Phi^{k-1} + (\rho + 1 - \delta) \cdot (\Phi + \delta - 1)^k\}}{(1 - \delta) \cdot \sqrt{(\rho + \Phi)^k \cdot (1 - \Phi - \delta)^k}} \quad \dots only\ for\ k \geq 2$

Solution for Case 2: patchy biofilm: [δ>(1 − Φ)]

$$\theta_n(\tau) = \alpha_n^* \cdot e^y \cdot \sum_{k=0}^{\infty} \beta_k^* \cdot I_{n+k}(x^*) \tag{81}$$

Where:

$x^* = 2 \cdot \tau \cdot \sqrt{(\rho + \Phi) \cdot (\Phi + \delta - 1)}$

$y = (1 - \rho - 2 \cdot \Phi - \delta) \cdot \tau$

$\alpha_0^* = 1$

$\alpha_n^* = \dfrac{\rho \cdot (\rho + \Phi)^{n-1}}{\sqrt{(\rho + \Phi)^n \cdot (\Phi + \delta - 1)^n}} \ \dots only\ for\ n \geq 1$

$\beta_0^* = 1$

$\beta_1^* = \dfrac{(2 \cdot \Phi + \delta - 1)}{\sqrt{(\rho + \Phi) \cdot (\Phi + \delta - 1)}}$

$\beta_k^* = \dfrac{\{[\rho \cdot (1 - \Phi - \delta) + \Phi \cdot (1 - \delta)] \cdot \Phi^{k-1} + (\rho + 1 - \delta) \cdot (\Phi + \delta - 1)^k\}}{(1 - \delta) \cdot \sqrt{(\rho + \Phi)^k \cdot (\Phi + \delta - 1)^k}} \quad \dots only\ for\ k \geq 2$

Solution for Case 3: border case between Cases 1 and 2: [δ = (1 − Φ)]

$$\theta_0(\tau) = e^{-\rho\tau} \tag{82(0)}$$

$$\theta_n(\tau) = e^{-(\rho + \Phi) \cdot \tau} \cdot \frac{\rho \cdot (\rho + \Phi)^{n-1}}{\Phi^n} \left\{ e^{\Phi\tau} - \sum_{k=0}^{n-1} \frac{(\tau \cdot \Phi)^k}{k!} \right\} \dots for\ (n>0) \tag{82(n)}$$

We provide the demonstration of these three solutions respectively in Appendix A, Appendix B and Appendix C. The consistency and coherence demonstrated when transformation between the solutions of the three analysed cases are carried out, considering in each transformation the appropriate mathematics modifications, allows to conclude that a unique recurrent algorithm is enough for all three applications. In fact, the solution of Case 1 conglobates the other two, after suitable modifications.

Part III
Miller Generalized Algorithm (eroding mathematical intractability)

7. Preliminary introduction.

The solution reached in Part II for the "Mono-layered concentrated growth" kinetics, defined by formulas (80) for continuous biofilm (Case 1) and by (81) for patchy biofilm (Case 2) are much more difficult to handle than the frontier between those two (Case 3) given by (82(0)) and (82(n)). Besides the Case 3 is the less important, representing only a very specific choice of parameters with the purpose of corroborate the mathematical coherence in all the deductions reached.

From these proof we concluded that to handle Case 1 solution (80), leads to a mathematical difficulty similar to handle Case 2 solution (81). And also leads to the same recurrent result.

Consequently we focus now our attention exclusively in continuous biofilm solution (80).

This solution is not easy to handle for numeric calculation and therefore also not easy for graphic and intelligible representation of the model. The solution obtained is complex because it consists of an infinite series of terms and the main difficulty lies on the fact that each term, in the infinite sum, contains a Bessel function of first kind, $J_{n+k}(x)$.

It is not because the summation is infinite in the number of terms why it is difficult reach a rigorous calculation. The truth is that terms of bigger order will always diminish in absolute value, and this circumstance allows, sooner or later, to despise those upper order terms thus becoming possible to accomplish all the computation without error.

The main problem to solve refers to the rigorous calculation of each Bessel function not only because extensive ranges of orders $(n + k)$ are required but also because their argument values, proportional with dimensionless time (τ), must vary over a large interval. As a matter of fact, we do not always find values for arguments that, in our case, are (or can be) relatively high. It is not possible to analyze a transient dynamic with limitations in the time scale because the value of the variable time that will allow us to have a complete view of the process is not known in advance. A priori do not exist tables providing such exigent demands on Bessel function orders and argument values.

The infinite series of terms with Bessel functions, which we have obtained in our case, can´t (or should not) be calculated using published tables, not only because it is necessary to use very high order functions, not always tabulated, but also because, even if the tables have these high order Bessel functions, the accuracy usually is not the same as the lower-order functions ($J_0(x)$, $J_1(x)$, $J_2(x)$, …).

This is an additional inconvenient question related to the lack of accuracy uniformity in data provided by known tables. Bessel functions of lower order (0, 1, 2, …) usually are tabulated with much more decimal significant places than the others (Abramowitz and Stegun, [21]). Thus, when one intends to calculate some more terms in the series, to avoid neglect still significant terms, coherence is lost because their accuracy is almost always inferior than that of the initial terms.

Consequently we must work only with computer tools paying attention to achieve the better exactitude disposable nowadays. We choose to compute in Excel spreadsheet not only because it stores numerical values as "Double Precision Floating Point", representing numbers accurate to something like 15 decimal places, but also because it allows to design the layout of the algorithms, over the spreadsheet with great personalized liberty.

Another important advantage lies on the fact that one can "see" the contents of each cell and easily detect and correct errors and (or) improve the global efficiency of the entire algorithm.

Once the numerical values published in these tables are discarded, our attention turns to the theoretical method used, in past times, to construct such tables of Bessel functions.

The central and fundamental tool for such purpose was the Three Terms Recurrence (TTR) Miller´s algorithm (Miller, [22]).

The immediate obvious way to solve the problem, of handle solution (80) with adequate accuracy, is to apply TTR Miller´s algorithm, term by term, till reach a Bessel function order high enough for neglect the absolute value of such term and also the absolute values of all following terms.

Another, more efficient and elegant, alternative concerns with considering all the infinite series summation, and so all the function $\theta_n(\tau)$, as a special function passible for application of an algorithm related to, but more general than, TTR Miller´s algorithm.

In more explicit words: functions $\theta_n(\tau)$ will came into play relatively to this new algorithm in a similar way Bessel functions of first kind play their role relatively to the already known TTR Miller´s algorithm. Application of this new approach implies, as first step, the deduction of a corresponding homogeneous recurrence for the special functions $\theta_n(\tau)$.

In the following section we will deduce that homogeneous recurrence and explain how can it be used for accurate computation of functions $\theta_n(\tau)$, translating to this new method a similar reasoning to that one of the old TTR Miller´s algorithm method.

These two methods can be jointly, and independently, applied and so we will be able to validate mutually both.

8. Generalized Miller´s like algorithm construction.

The calculation of the model equation (80), will be done, in this section, applying a method alike that of Miller [22] but more general.

This method applies to the so-called Special Functions when one can construct recurrence formulas between them. Knowing the functions of lower orders we can calculate those of higher orders with a formula of progressive recurrence and vice versa with a regressive one.

However, if the Special Functions are decreasing when their order increases the application of the progressive recurrence will imply the use of the subtraction operation and the loss of significant numbers (S. Zhang and J. Jin, [23]) each time the recurrence computation applies, making the method numerically unstable.

This is the case for Bessel functions of first kind and therefore also the case for the functions $\theta_n(\tau)$ at the initial values of (τ). But not only in the initial values of (τ) since there will always exist surface fractions $\theta_n(\tau)$, in the largest orders (n) that are in stage of increasing its value, having therefore a low value, since the kinetic process is an overall continuous accumulation of biomass.

Therefore, it is necessary to use a regressive formula in all values of dimensionless time (τ). That is the same to say that we have to compute the functions $\theta_n(\tau)$ with the smallest orders (n) depending of those ones with the biggest orders (n).

Miller [22] solved the problem by assigning an arbitrary value to the function where the recurrence calculation starts, which is the highest order function (n) of all of them.

By applying the homogeneous recurrence formula one gets the relative correct magnitudes between all the functions under calculation. After a suitable common normalization factor must be applied to all the functions of the sequence. The result of this multiplication is the exact value of all and each one of the functions. The aforesaid suitable common normalization factor is defined by the known value, in the particular case under analysis, of an infinite series with form,

$$\sum_{n=0}^{\infty} c_n \cdot f_n(\tau)$$

(83)

The homogeneous recurrence formula to be constructed must, for the functions $\theta_n(\tau)$, read like,

$$\theta_n(\tau) = F[\,\theta_{n+1}(\tau), \theta_{n+2}(\tau), \dots, \theta_{n+k}(\tau)]$$

... where,

$$k \geq 1$$

(84)

... and being $\theta_n(\tau)$ obtained depending of $\theta_{n+1}(\tau), \theta_{n+2}(\tau), \dots, \dots$ and $\theta_{n+k}(\tau)$. We call (84) a $(k+1)$-terms homogeneous recurrence.

Let´s deduce now the homogeneous recurrence, and for start, let define the auxiliary functions $W_n(x)$, for $(n \geq 0)$,

$$W_n(x) = \sum_{k=0}^{\infty} \beta_k \cdot J_{n+k}(x)$$

$(85 - A)$

$$W_n(x) = \beta_0 \cdot J_n(x) + \beta_1 \cdot J_{n+1}(x) + \sum_{k=2}^{\infty} \beta_k \cdot J_{n+k}(x)$$

$(85 - B)$

... where coefficients β_k are defined like they have been defined in the model equation (80),

$$\beta_k = \begin{cases} 1 \dots if\ k = 0 \\ \\ \frac{b_{k-1}}{\gamma^k} \dots if\ k \geq 1 \end{cases} \qquad \dots being,\ \gamma = \sqrt{(1 - \Phi - \delta) \cdot (\rho + \Phi)}\ \dots and,\ b_k = c_k \cdot k!$$

(86)

Following a brief revision from Appendix A, coefficients c_k are, in their turn, defined by equations $(A19(0))$ and $(A29)$,

$$c_k = \begin{cases} (2 \cdot \Phi + \delta - 1)\ \dots if\ k = 0 & (A19(0)) \\ \\ \dfrac{\{[\rho \cdot (1 - \Phi - \delta) + \Phi \cdot (1 - \delta)] \cdot \Phi^k + (\rho + 1 - \delta) \cdot (\Phi + \delta - 1)^{k+1}\}}{(1 - \delta) \cdot k!}\ \dots if\ k \geq 1 & (A29) \end{cases}$$

And, also from Appendix A, consequently the coefficients b_k obey equation $(A20)$,

$$b_{k+2} + A \cdot b_{k+1} + B \cdot b_k = 0 \quad \dots with\ (k \geq 0)$$

(A20)

... where,

$$A = (1 - 2 \cdot \Phi - \delta)$$

(A22)

$$B = \Phi \cdot (\Phi + \delta - 1)$$

(A23)

Let use functions $W_n(x)$ in the form,

$$W_n(x) = J_n(x) + \sum_{k=1}^{\infty} \frac{b_{k-1}}{\gamma^k} \cdot J_{n+k}(x)$$

(87)

Our purpose is now to obtain a recurrence relation between the functions $W_n(x)$ in which the functions $J_n(x)$ are not present. And, in the sequel, applying the relationship between functions $W_n(x)$ and functions $\theta_n(\tau)$, that recurrence will be easily converted into a recurrence between the functions $\theta_n(\tau)$, as desired. Recurrences concerning Bessel functions of first kind imply $J_n(x)$, $J_{n+1}(x)$ and $J_{n+2}(x)$. For this reason let now write explicitly $W_n(x)$, $W_{n+1}(x)$ and $W_{n+2}(x)$ in the following way,

$$W_n(x) = J_n(x) + \frac{b_0}{\gamma} \cdot J_{n+1}(x) + \frac{b_1}{\gamma^2} \cdot J_{n+2}(x) + \sum_{k=3}^{\infty} \frac{b_{k-1}}{\gamma^k} \cdot J_{n+k}(x)$$

$$(88(0))$$

$$W_{n+1}(x) = J_{n+1}(x) + \frac{b_0}{\gamma} \cdot J_{n+2}(x) + \sum_{k=2}^{\infty} \frac{b_{k-1}}{\gamma^k} \cdot J_{n+k+1}(x)$$

$$(88(1))$$

$$W_{n+2}(x) = J_{n+2}(x) + \sum_{k=1}^{\infty} \frac{b_{k-1}}{\gamma^k} \cdot J_{n+k+2}(x)$$

$$(88(2))$$

Remodelling the summations so that everyone starts with $(k = 1)$ we obtain,

$$W_n(x) = J_n(x) + \frac{b_0}{\gamma} \cdot J_{n+1}(x) + \frac{b_1}{\gamma^2} \cdot J_{n+2}(x) + \sum_{k=1}^{\infty} \frac{b_{k+1}}{\gamma^{k+2}} \cdot J_{n+k+2}(x)$$

$$(89(0))$$

$$W_{n+1}(x) = J_{n+1}(x) + \frac{b_0}{\gamma} \cdot J_{n+2}(x) + \sum_{k=1}^{\infty} \frac{b_k}{\gamma^{k+1}} \cdot J_{n+k+2}(x)$$

$$(89(1))$$

$$W_{n+2}(x) = J_{n+2}(x) + \sum_{k=1}^{\infty} \frac{b_{k-1}}{\gamma^k} \cdot J_{n+k+2}(x)$$

$$(89(2))$$

Now we properly multiply (89(1)) and (89(2)) in such a way that, by associating the same Bessel function in the three equations (89(0)), (89(1)) and (89(2)), equality (A20) can be used thus eliminating the infinite terms summation:

$$W_n(x) = J_n(x) + \frac{b_0}{\gamma} \cdot J_{n+1}(x) + \frac{b_1}{\gamma^2} \cdot J_{n+2}(x) + \sum_{k=1}^{\infty} \frac{b_{k+1}}{\gamma^{k+2}} \cdot J_{n+k+2}(x)$$

$$(90(0))$$

$$\frac{A}{\gamma} \cdot W_{n+1}(x) = \frac{A}{\gamma} \cdot J_{n+1}(x) + \frac{A \cdot b_0}{\gamma^2} \cdot J_{n+2}(x) + \sum_{k=1}^{\infty} \frac{A \cdot b_k}{\gamma^{k+2}} \cdot J_{n+k+2}(x)$$

$$(90(1))$$

$$\frac{B}{\gamma^2} \cdot W_{n+2}(x) = \frac{B}{\gamma^2} \cdot J_{n+2}(x) + \sum_{k=1}^{\infty} \frac{B \cdot b_{k-1}}{\gamma^{k+2}} \cdot J_{n+k+2}(x)$$

$$(90(2))$$

Adding the three equations (90(0)), (90(1)) and (90(2)) we obtain,

$$W_n(x) + \frac{A}{\gamma} \cdot W_{n+1}(x) + \frac{B}{\gamma^2} \cdot W_{n+2}(x) = J_n(x) + \frac{(b_0 + A)}{\gamma} \cdot J_{n+1}(x) +$$

$$+ \frac{(b_1 + A \cdot b_0 + B)}{\gamma^2} \cdot J_{n+2}(x) + \sum_{k=1}^{\infty} \frac{(b_{k+1} + A \cdot b_k + B \cdot b_{k-1})}{\gamma^{k+2}} \cdot J_{n+k+2}(x)$$

$$(91)$$

Observing that, from $b_k = c_k \cdot k!$, and also $(A19\,(0))$, $(A19\,(1))$, $(A22)$ and $(A23)$, the following three equalities are valid,

$b_0 + A = 0$

(92)

$b_1 + A \cdot b_0 + B = \gamma^2$

(93)

$b_{k+1} + A \cdot b_k + B \cdot b_{k-1} = 0 \quad \dots \; for \; (k \geq 1)$ (94)

... we are now able to insert they in (91) , and therefore getting in it a great simplification,

$$W_n(x) + \frac{A}{\gamma} \cdot W_{n+1}(x) + \frac{B}{\gamma^2} \cdot W_{n+2}(x) = J_n(x) + J_{n+2}(x)$$ (95)

Let now add 2 in the discrete order (n) at (95),

$$W_{n+2}(x) + \frac{A}{\gamma} \cdot W_{n+3}(x) + \frac{B}{\gamma^2} \cdot W_{n+4}(x) = J_{n+2}(x) + J_{n+4}(x)$$ (96)

... and call into play the identities,

$$J_n(x) + J_{n+2}(x) = \frac{2 \cdot (n+1)}{x} \cdot J_{n+1}(x)$$ (97(0))

$$J_{n+2}(x) + J_{n+4}(x) = \frac{2 \cdot (n+3)}{x} \cdot J_{n+3}(x)$$ (97(2))

... which must be substituted in (95) and (96),

$$W_n(x) + \frac{A}{\gamma} \cdot W_{n+1}(x) + \frac{B}{\gamma^2} \cdot W_{n+2}(x) = \frac{2 \cdot (n+1)}{x} \cdot J_{n+1}(x)$$ (98)

$$W_{n+2}(x) + \frac{A}{\gamma} \cdot W_{n+3}(x) + \frac{B}{\gamma^2} \cdot W_{n+4}(x) = \frac{2 \cdot (n+3)}{x} \cdot J_{n+3}(x)$$ (99)

... reducing this way to only one the Bessel functions of first kind figured in the right hand sides. Now we explicit those Bessel functions in the left hand side,

$$J_{n+1}(x) = \frac{x}{2 \cdot (n+1)} \cdot \left\{ W_n(x) + \frac{A}{\gamma} \cdot W_{n+1}(x) + \frac{B}{\gamma^2} \cdot W_{n+2}(x) \right\}$$ (100)

$$J_{n+3}(x) = \frac{x}{2 \cdot (n+3)} \cdot \left\{ W_{n+2}(x) + \frac{A}{\gamma} \cdot W_{n+3}(x) + \frac{B}{\gamma^2} \cdot W_{n+4}(x) \right\}$$ (101)

Back to equation (95) let write it again but adding this time 1 in the discrete order (n),

$$W_{n+1}(x) + \frac{A}{\gamma} \cdot W_{n+2}(x) + \frac{B}{\gamma^2} \cdot W_{n+3}(x) = J_{n+1}(x) + J_{n+3}(x)$$ (102)

The right hand side of (102) only depends on $J_{n+1}(x)$ and $J_{n+3}(x)$ which in turn are given by (100) and (101) depending only on $W_{n+k}(x)$ with $k = 0, 1, 2, 3$ or 4. Inserting the equations (100) and (101) in the right hand side of (102) we obtain an equation where all Bessel functions of first kind have been eliminated by suitable substitutions, as desired.

That result reads,

$$W_{n+1}(x) + \frac{A}{\gamma} \cdot W_{n+2}(x) + \frac{B}{\gamma^2} \cdot W_{n+3}(x) =$$

$$= \frac{x}{2 \cdot (n+1)} \cdot \left\{ W_n(x) + \frac{A}{\gamma} \cdot W_{n+1}(x) + \frac{B}{\gamma^2} \cdot W_{n+2}(x) \right\} +$$

$$+ \frac{x}{2 \cdot (n+3)} \cdot \left\{ W_{n+2}(x) + \frac{A}{\gamma} \cdot W_{n+3}(x) + \frac{B}{\gamma^2} \cdot W_{n+4}(x) \right\}$$

$$(103)$$

The expression we have reached, (103), can now be transformed into a progressive recurrence if we explicit $W_{n+4}(x)$ as depending of the functions of lesser orders, or in a regressive recurrence if we explicit $W_n(x)$ as depending of all the others which have higher orders. For the sake to attain numerical stability we are interested in the regressive recurrence for a proper application of the Generalized Miller´s like algorithm we seek for construction.

Before manipulate (103) is convenient establish an alternative expression for $\left(\frac{2}{x} \right)$.

From the definitions $x = 2 \cdot \tau \cdot \sqrt{(\rho + \Phi) \cdot (1 - \Phi - \delta)}$ and $\gamma = \sqrt{(\rho + \Phi) \cdot (1 - \Phi - \delta)}$ the result follows immediately,

$$\frac{2}{x} = \frac{1}{\gamma \cdot \tau}$$

$$(104)$$

The wanted regressive recurrence is now reached easily from (103), taking (104) in consideration,

$$W_n(x) = \left[\frac{(n+1)}{\gamma \cdot \tau} - \frac{A}{\gamma} \right] \cdot W_{n+1}(x) + \left[\frac{(n+1) \cdot A}{\gamma^2 \cdot \tau} - \frac{B}{\gamma^2} - \frac{(n+1)}{(n+3)} \right] \cdot W_{n+2}(x) +$$

$$+ \left[\frac{(n+1) \cdot B}{\gamma^3 \cdot \tau} - \frac{(n+1) \cdot A}{(n+3) \cdot \gamma} \right] \cdot W_{n+3}(x) - \frac{(n+1) \cdot B}{(n+3) \cdot \gamma^2} \cdot W_{n+4}(x) \qquad (105)$$

What logically follows must be to relate functions $W_n(x)$ with functions $\theta_n(\tau)$ and then insert that relation in (105) and finally obtain a regressive recurrence for these last one functions. From the model solution, (80) and the definition of $W_n(x)$, (87), we write,

$$\theta_0(\tau) = e^y \cdot W_0(x)$$

$$(106(0))$$

$$\theta_n(\tau) = \frac{\rho \cdot (\rho + \Phi)^{n-1}}{\gamma^n} \cdot e^y \cdot W_n(x) \quad \dots \ for \ (n \geq 1)$$

$$(106(n))$$

Next step is to obtain explicit formulas for $W_n(x)$ depending on $\theta_n(\tau)$,

$$W_0(x) = e^{-y} \cdot \theta_0(\tau)$$

$$(107(0))$$

$$W_n(x) = e^{-y} \cdot \frac{\gamma^n}{\rho \cdot (\rho + \Phi)^{n-1}} \cdot \theta_n(\tau) \dots for \ (n \geq 1)$$

$$(107(n))$$

Regarding the fact that the function $W_0(x)$ has a dependence, different from all the others, on the corresponding function $\theta_0(\tau)$ one is compelled to conclude that also a different and unique regressive recurrence relation must be established for $\theta_0(\tau)$. Accordingly, inserting (107(0)) and (107(n)) in (105), and making $(n = 0)$, the recurrence for $\theta_0(\tau)$ is achieved and reads,

$$\theta_0(\tau) = \left[\frac{1}{\tau} - A \right] \cdot \frac{\theta_1(\tau)}{\rho} + \left[\frac{A}{\tau} - B - \frac{\gamma^2}{3} \right] \cdot \frac{\theta_2(\tau)}{\rho \cdot (\rho + \Phi)} +$$

$$+ \left[\frac{B}{\tau} - \frac{A \cdot \gamma^2}{3} \right] \cdot \frac{\theta_3(\tau)}{\rho \cdot (\rho + \Phi)^2} - \frac{B \cdot \gamma^2}{3} \cdot \frac{\theta_4(\tau)}{\rho \cdot (\rho + \Phi)^3} \qquad (108(0))$$

… and inserting only (107(n)) in (105), and making $(n \geq 1)$, we reach the formula that allows the regressive computation of all the others $\theta_n(\tau)$,

$$\theta_n(\tau) = \left[\frac{(n+1)}{\tau} - A \right] \cdot \frac{\theta_{n+1}(\tau)}{(\rho + \Phi)} + \left[\frac{(n+1) \cdot A}{\tau} - B - \frac{(n+1) \cdot \gamma^2}{(n+3)} \right] \cdot \frac{\theta_{n+2}(\tau)}{(\rho + \Phi)^2} +$$

$$+\left[\frac{(n+1)\cdot B}{\tau}-\frac{(n+1)\cdot A\cdot\gamma^2}{(n+3)}\right]\cdot\frac{\theta_{n+3}(\tau)}{(\rho+\Phi)^3}-\frac{(n+1)\cdot B\cdot\gamma^2}{(n+3)}\cdot\frac{\theta_{n+4}(\tau)}{(\rho+\Phi)^4} \qquad (108(n))$$

The last two regressive recurrences, $(108(0))$ and $(108(n))$ can be clustered in only one, which reads like,

General regressive recurrence for functions $\theta_n(\tau)$ (biofilm early stages formation and growth model)

$$\theta_n(\tau)=\left[\frac{(n+1)}{\tau}-A\right]\cdot\frac{\theta_{n+1}(\tau)}{D_1}+\left[\frac{(n+1)\cdot A}{\tau}-B-\frac{(n+1)\cdot C}{(n+3)}\right]\cdot\frac{\theta_{n+2}(\tau)}{D_2}+$$

$$+\left[\frac{(n+1)\cdot B}{\tau}-\frac{(n+1)\cdot A\cdot C}{(n+3)}\right]\cdot\frac{\theta_{n+3}(\tau)}{D_3}-\frac{(n+1)\cdot B\cdot C}{(n+3)}\cdot\frac{\theta_{n+4}(\tau)}{D_4} \qquad (109)$$

Where:

$A=(1-2\cdot\Phi-\delta)$

$B=\Phi\cdot(\Phi+\delta-1)$

$C=(\rho+\Phi)\cdot(1-\Phi-\delta)$

$D_k=\begin{cases}\rho\cdot[\rho+\Phi)^{k-1}\ \dots for\ (n=0)\\[6pt]\\ (\rho+\Phi)^k\qquad\dots for\ (n\geq1)\end{cases}$ $\dots k\ in\ the\ range:\quad (1\leq k\leq4)$

Remark: The designation "General" for this recurrence means that it is valid in the three cases analysed in the Appendixes A, B, and C, in Part II:

Case 1: Continuous Biofilm $[\delta<(1-\Phi)]$

Case 2: Patchy Biofilm $[\delta>(1-\Phi)]$

Case 3: Frontier between Continuous and Patchy Biofilm $[\delta=(1-\Phi)]$

Our goal is to apply correctly alike ideas to those applied by Miller [22] but now with this five terms recurrence (FTR) instead of the already known three term recurrence (TTR) classical algorithm.

For start, formula $(108(n))$ is applied at an order $(n+4)$ high enough to allow us to set $\theta_{n+4}(\tau)=0$, $\theta_{n+3}(\tau)=0$ and $\theta_{n+2}(\tau)=0$. That´s to say: these orders, $(n+4)$, $(n+3)$ and $(n+2)$, must be so high that the corresponding fractions of solid support area $\theta_{n+4}(\tau)$, $\theta_{n+3}(\tau)$ and $\theta_{n+2}(\tau)$ represent, in their turn, an accumulation of pilled layers so big that was not yet achieved at any point in the biofilm, at the value of dimensionless time (τ) under consideration.

In the same formula, $(108(n))$, a value of 1 must be assigned to $\theta_{n+1}(\tau)$ if we follow strictly Miller´s criterion (Miller [22]). However we introduce in this stage an improvement consisting in assign to $\theta_{n+1}(\tau)$ a small positive value, ε_{n+1}, but not necessarily equal to 1, and preferably less than 1. This allows a more conservative increase in absolute values of the successive $\theta_{n-k}(\tau)$ under computation avoiding to reach the upper absolute value limit of Excel, which is 10^{+308}, or, in inverse reasoning, allows start the recurrence in higher orders $(n+4)$, $(n+3)$ and $(n+2)$ accomplishing this way computations much more extensive in their number of recurrent steps.

So, the first recurrent computation consists in doing $\theta_{n+4}(\tau)=0$, $\theta_{n+3}(\tau)=0$, $\theta_{n+2}(\tau)=0$ and $\theta_{n+1}(\tau)=\varepsilon_{n+1}$ where $(0<\varepsilon_{n+1}\leq1)$, insert these values in $(108(n))$, and so get the non normalized value of $\theta_n(\tau)$, which we designate by ε_n.

The second recurrent computation consists in apply once again $(108(n))$, but diminishing 1 to all orders $(n \pm k)$. We designate by $(108(n-1))$ such "new" equation,

$$\theta_{n-1}(\tau) = \left[\frac{(n)}{\tau} - A\right] \cdot \frac{\theta_n(\tau)}{(\rho+\Phi)} + \left[\frac{(n)\cdot A}{\tau} - B - \frac{(n)\cdot\gamma^2}{(n+2)}\right] \cdot \frac{\theta_{n+1}(\tau)}{(\rho+\Phi)^2} +$$

$$+ \left[\frac{(n)\cdot B}{\tau} - \frac{(n)\cdot A\cdot\gamma^2}{(n+2)}\right] \cdot \frac{\theta_{n+2}(\tau)}{(\rho+\Phi)^3} - \frac{(n)\cdot B\cdot\gamma^2}{(n+2)} \cdot \frac{\theta_{n+3}(\tau)}{(\rho+\Phi)^4} \qquad (108(n-1))$$

Now we insert the former values of $\theta_{n+3}(\tau) = 0$, $\theta_{n+2}(\tau) = 0$, $\theta_{n+1}(\tau) = \varepsilon_{n+1}$ and $\theta_n(\tau) = \varepsilon_n$ and obtain the non normalized value of $\theta_{n-1}(\tau)$, coherently designated by ε_{n-1}.

This procedure is done repeatedly $(n-2)$ more times till the non normalized value of $\theta_1(\tau)$, designed ε_1, is calculated.

In general, the k-th recurrent computation, being $(1 \le k \le n)$, is realized with equation $(108(n-k+1))$, which reads,

$$\theta_{n-k+1}(\tau) = \left[\frac{(n-k+2)}{\tau} - A\right] \cdot \frac{\theta_{n-k+2}(\tau)}{(\rho+\Phi)} + \left[\frac{(n-k+2)\cdot A}{\tau} - B - \frac{(n-k+2)\cdot\gamma^2}{(n-k+4)}\right] \cdot \frac{\theta_{n-k+3}(\tau)}{(\rho+\Phi)^2} +$$

$$+ \left[\frac{(n-k+2)\cdot B}{\tau} - \frac{(n-k+2)\cdot A\cdot\gamma^2}{(n-k+4)}\right] \cdot \frac{\theta_{n-k+4}(\tau)}{(\rho+\Phi)^3} - \frac{(n-k+2)\cdot B\cdot\gamma^2}{(n-k+4)} \cdot \frac{\theta_{n-k+5}(\tau)}{(\rho+\Phi)^4}$$

$$(108(n-k+1))$$

The four initial postulated values, $\theta_{n+4}(\tau) = 0$, $\theta_{n+3}(\tau) = 0$, $\theta_{n+2}(\tau) = 0$ and $\theta_{n+1}(\tau) = \varepsilon_{n+1}$ are used in the first recurrent computation. Then, from these, the three values $\theta_{n+3}(\tau) = 0$, $\theta_{n+2}(\tau) = 0$ and $\theta_{n+1}(\tau) = \varepsilon_{n+1}$, are still necessary in the second recurrent computation. In the same way, the two values $\theta_{n+2}(\tau) = 0$ and $\theta_{n+1}(\tau) = \varepsilon_{n+1}$ are needed for the third computation, and also the value $\theta_{n+1}(\tau) = \varepsilon_{n+1}$ still for the fourth one. In the fifth and subsequent recurrent computations only calculated values in former computations are needed. None of the initial fourth postulated values figures anymore.

In all this regressive and recurrent computations, equations $(108(n))$, $(108(n-1))$, $(108(n-2))$, ... , $(108(n-k+1))$, ... , $(108(3))$, $(108(2))$ and $(108(1))$ are applied and the non normalized values of $\theta_n(\tau)$, $\theta_{n-1}(\tau)$, $\theta_{n-2}(\tau)$, ... , $\theta_{n-k+1}(\tau)$, ... , $\theta_3(\tau)$, $\theta_2(\tau)$ and $\theta_1(\tau)$ are respectively obtained.

Lastly, the non normalized value of $\theta_0(\tau)$, is computed applying equation $(108(0))$ inserting in it the non normalized values of $\theta_1(\tau)$, $\theta_2(\tau)$, $\theta_3(\tau)$ and $\theta_4(\tau)$ obtained, respectively, in the former n-th, $(n-1)$-th, $(n-2)$-th and $(n-3)$-th recurrent computations.

In the following Table 1 all the sequence of these recurrent computations for the non normalized values of all the functions $\theta_k(\tau)$, being $(0 \le k \le n+4)$, is succinctly and clearly explained.

Till this stage we only have the non normalized values of all functions $\theta_k(\tau)$. Opportunely we now recall that they relative proportions are already correct.

In the sequel we must add up all those non normalized values and divide all of them by the value of that summation, which, in this way, works like a normalization factor, because the summation of all the fractions $\theta_k(\tau)$ must be equal to 1.

The initial postulated order, from where the recurrent computations must begin to be applied, ought to be large enough for the positive, non normalized, value assigned to $\theta_{n+1}(\tau)$ be much lower or, at least, alike to the reached, non normalized value of $\theta_0(\tau)$, at the other extreme of the entire computation. This last scenario is only valid if $\theta_0(\tau)$ attained already very low values as consequence of having elapsed enough time since the beginning at $(\tau = 0)$ and, therefore, almost support area is just at hand to be completely covered.

In other words: the highest order $(n + 1)$ among all the $\theta_k(\tau)$ computed and, so, considered not null must be high enough to realty represent a $\theta_k(\tau)$ with a positive value, but very low, very near to zero. Only this way the postulated null values of $\theta_{n+2}(\tau)$, $\theta_{n+3}(\tau)$, $\theta_{n+4}(\tau)$, and beyond that can be considered correctly valued. The aforesaid need for start the recurrent computations in an order $(n + 4)$ that can be very high directs us to the new problem of avoid that the maximum value of the non normalized functions $\theta_k(\tau)$ don´t have an absolute value so high that exceeds the positive numerical limit of Excel spreadsheet. This limit has already been mentioned and is around 10^{+308}. From our numerical experiments we concluded that this big upper positive limit conjugated with the possibility of start with a postulated value for $\theta_{n+1}(\tau)$ very low, albeit still positive, $(\varepsilon_{n+1} \gtrsim 0)$, leads always, meaning this for all values of dimensionless time (τ), to a possible complete and accurate computation of all the functions $\theta_k(\tau)$.

Logically, as the dimensionless time (τ) increases, more and more fractions $\theta_k(\tau)$, with higher order (k) must be calculated because they represent already absolute positive values not anymore negligible.

Consequently once fixed the model parameters values, in a numerical experiment, as time (τ) increases a successive need for start the algorithm in an order $(n + 4)$ higher, and higher again, come into play. Facing this circumstance the accurate recurrent computation of the kinetic evolution, over a broad range of time $(\tau \geq 0)$, will always imply the construction of a series of similar Generalized Miller´s like algorithms in the same spreadsheet, but where the starting computation order $(n + 4)$ increases from one to the next algorithm. Bigger values of time (τ) demand bigger initial $(n + 4)$ orders as the natural consequence of the physical growth of the biofilm, with the continuous accumulation of biomass and concomitant attaining of fractions at solid support area covered by more and more pilled layers.

Table 1

Computation nº/ /Applied equation	Not normalized input values:				Result
1 (∗) **(108(n))**	$\theta_{n+4}(\tau)$	$\theta_{n+3}(\tau)$	$\theta_{n+2}(\tau)$	$\theta_{n+1}(\tau)$	$\theta_n(\tau)$
	0	0	0	$0 < \varepsilon_{n+1} \leq 1$	ε_n
2 (∗) **(108($n-1$))**	$\theta_{n+3}(\tau)$	$\theta_{n+2}(\tau)$	$\theta_{n+1}(\tau)$	$\theta_n(\tau)$	$\theta_{n-1}(\tau)$
	0	0	$0 < \varepsilon_{n+1} \leq 1$	ε_n	ε_{n-1}
3 (∗) **(108($n-2$))**	$\theta_{n+2}(\tau)$	$\theta_{n+1}(\tau)$	$\theta_n(\tau)$	$\theta_{n-1}(\tau)$	$\theta_{n-2}(\tau)$
	0	$0 < \varepsilon_{n+1} \leq 1$	ε_n	ε_{n-1}	ε_{n-2}
	....	....	....	....	....
....	....	....	....	....	....
k (∗) **(108($n-k+1$))**	$\theta_{n-k+5}(\tau)$	$\theta_{n-k+4}(\tau)$	$\theta_{n-k+3}(\tau)$	$\theta_{n-k+2}(\tau)$	$\theta_{n-k+1}(\tau)$
	ε_{n-k+5}	ε_{n-k+4}	ε_{n-k+3}	ε_{n-k+2}	ε_{n-k+1}
	....	....	....	....	....
....	....	....	....	....	....
$n-2$ (∗)	$\theta_7(\tau)$	$\theta_6(\tau)$	$\theta_5(\tau)$	$\theta_4(\tau)$	$\theta_3(\tau)$

(108(3))	ε_7	ε_6	ε_5	ε_4	ε_3
$n-1$ (*)	$\theta_6(\tau)$	$\theta_5(\tau)$	$\theta_4(\tau)$	$\theta_3(\tau)$	$\theta_2(\tau)$
(108(2))	ε_6	ε_5	ε_4	ε_3	ε_2
n (*)	$\theta_5(\tau)$	$\theta_4(\tau)$	$\theta_3(\tau)$	$\theta_2(\tau)$	$\theta_1(\tau)$
(108(1))	ε_5	ε_4	ε_3	ε_2	ε_1
$n+1$ (**)	$\theta_4(\tau)$	$\theta_3(\tau)$	$\theta_2(\tau)$	$\theta_1(\tau)$	$\theta_0(\tau)$
(108(0))	ε_4	ε_3	ε_2	ε_1	ε_0

Short legend

(*) $-$**Regressive Recurrences used in the computations numbers** (k), **with** $(1 \leq k \leq n)$ /
/ **Recurrent equation** $(108(k))$

(**) $-$**Regressive Recurrence used in the computation number** $(n+1)$/
/**Recurrent equation** $(108(0))$

Part IV

8. Numerical examples

The model parameters are $L \geq 1$, $\rho > 0$, $0 \leq \phi \leq 1$ and $\delta \geq 0$ but, in this work, we limited the analysis to the simplified version with $L = 1$.

In Fig. 4 the possible values of ɸ and δ divide the graph into two zones: the triangle ΔACI, corresponding to continuous biofilm, and the zone between $\phi = 0$ and $\phi = 1$ and above line CI, corresponds to patchy biofilm. Borderline case corresponds to points in line CI.
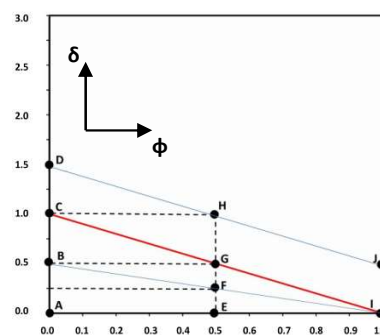
Fig. 4. Values of $0 \leq \phi \leq 1$ and $\delta \geq 0$

Continous biofilm: triângle ΔACI

Patchy biofilm: Between lines ϕ = 0

and ϕ = 1 and above line CI

Borderline: line CI

With the indicated points, numerical simulations can be made in order to obtain a sufficiently enlightening output. For each point, it seems reasonable to vary ρ between 0.001 (near zero) and 10 (much above 1). We will illustrate the model, for continuous biofilm, with points A and E and, for patchy biofilm, with point D.

In Fig. 5, 6 and 12, the functions $\theta n = \theta n(\tau)$ are represented for points A, E and D. In addition, Tables 2 and 3 contain numerical values that also illustrate the results obtained. Table 2 refers to the examples in Fig. 5 and 6, and Table 3 to those in Fig. 12.

In each one of the Fig. 5, 6 and 12 there are seven graphs corresponding, from left to right, and top to bottom, to the values of $\rho = 0.001, 0.01, 0.1, 0.2, 1, 5$ and 10. Numerical values were calculated using the algorithm described in Part III and have 12 decimal places.

In Fig. 5 ($\phi = 0$ and $\delta = 0$) the only processes are the arrival and attachment flow and the growth of bacteria in parallel to the solid support. Under these circumstances it is foreseeable that the time necessary for the solid support to be covered, at least, with one layer of bacteria decreases as ρ increases. In fact, the roots of $\theta_0(\tau) = 0$ decrease when ρ increases. It was also predictable that, with the increase of ρ, more overlap layers will form. Therefore, the biofilm will have more different local thicknesses. Fig 5 confirms this variety of thicknesses as the solid support becomes fully covered. For $\rho = 0.001$ the biofilm grows as a simple monolayer. At the other extreme, for $\rho = 10$, areas covered by 2, 3, up to 8 or 9 layers are locally formed before the solid support is fully covered.
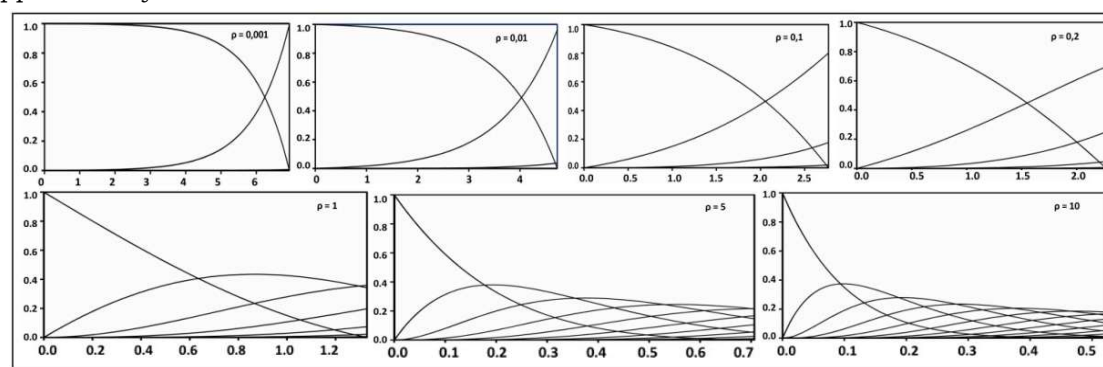
Fig. 5. $\theta_n(\tau)$ functions for $\phi = 0$ and $\delta = 0$.

In Fig. 6 ($\phi = 0.5$ and $\delta = 0$) the bacterial specific growth rate takes place in two directions, parallel and perpendicular to the solid support, the two components being of equal value. Now only half of the bacterial growth takes place in parallel to the solid support, which greatly delays its total coverage. In fact, for small ρ, full coverage is not achieved in reasonably not too long times. As in the examples in Fig 5, the time to obtain full coverage decreases when ρ increase. But the fact that these times are longer gives rise to a biofilm of more varied and irregular thicknesses than in the examples of Fig. 5, due to the vertical bacterial growth component.

In particular, for $\rho = 0.001$ and $\rho = 0.01$, there is no total coverage for very long times, which allows the model to still predict a patchy biofilm. For $\rho = 0.01$ it can be considered that the total coverage of the solid support has been approximately reached near $\tau = 200$. But from the mathematical point of view it was not: $\theta_0(200) = 0.018498843945$.
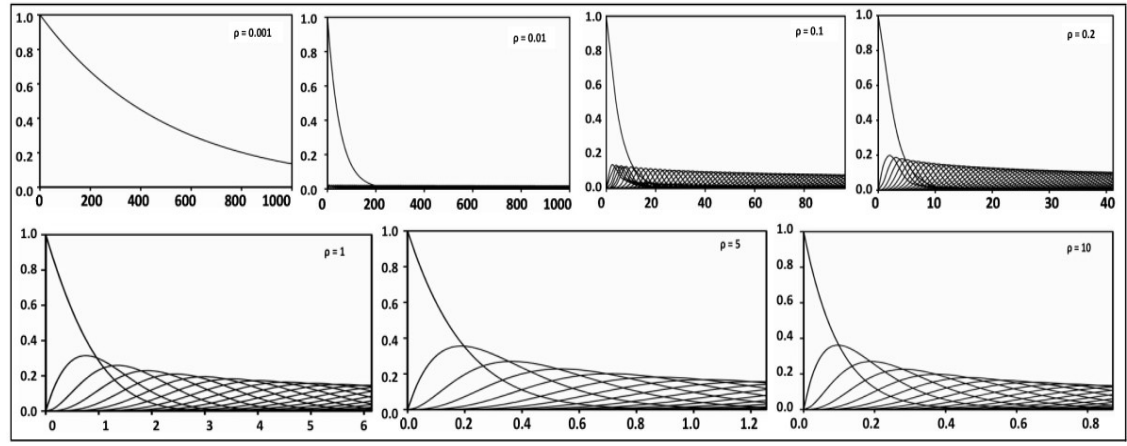
Fig. 6. $\theta_n(\tau)$ functions for ϕ = 0.5 and δ = 0.

In Fig 6. the graph for ρ = 0.001   looks something mysterious. In fact θ_0 decreases and, from τ = 0 to τ = 1000, no growth of any function $\theta_n(\tau)$ for $1 \leq n$ is observed. It seems that the covered fraction $[1 - \theta_0(\tau)]$ and,   in particular, $[1 - \theta_0(1000)] = 0.864529372893$ is missing. Fig. 7 unveils this mystery by clarifying that the fraction covered by one or more layers is made up of many tiny fractions of thickness from $n = 1$ (one layer) $to \; n \gg 1$ (innumerable layers). Those fractions are so tiny that their values can´t be seen in the plot.

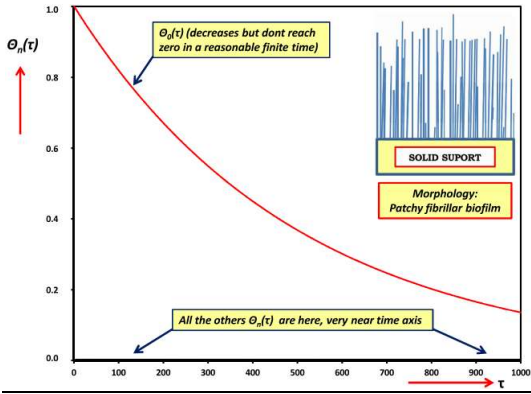| Table 2. Roots of $\theta_0(\tau)$ = 0		
ρ	Refers to Fig. 5, (ϕ = 0; δ = 0)	Refers to Fig.6, (ϕ = 0.5; δ = 0)
0.001	6.932827750718	$\tau \gg 1000$ [$\theta_0(1000)$ = 0.135470627107]
0.01	4.727171132161	$\tau \gg 1000$ [$\theta_0(1000)$ = 0.000000002074]
0.1	2.769187961061	96.579242354601
0.2	2.269779638644	41.187297039132
1	1.328742412285	6.143134095676
5	0.706340731785	1.254316614194
10	0.524959362087	0.871073346776

Fig. 7. Interpretation of plot from Fig. 6

(ρ = 0.001)

The beautiful close-ups of Figs 8 to 11 help to better clarify this example. Fig. 8 shows the functions $\theta_n(\tau)$ with $1 \le n \le 253$ (θ_0 is invisible).

The maximum capacity of Excel is approximately 254 functions in a single plot. The functions $\theta_n(\tau)$ for $n = 1, 43, 85, 127, 169, 211$ and 253 are equally spaced with respect to n, and they are represented in red for a better visualization of the shape of this whole set of functions. All the others were represented in gray and, because they are so close, they seem to have filled the entire space. However this space represents the close-up only up to just $\tau = 200$.
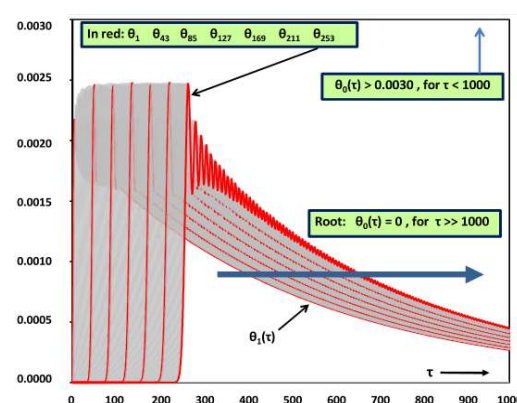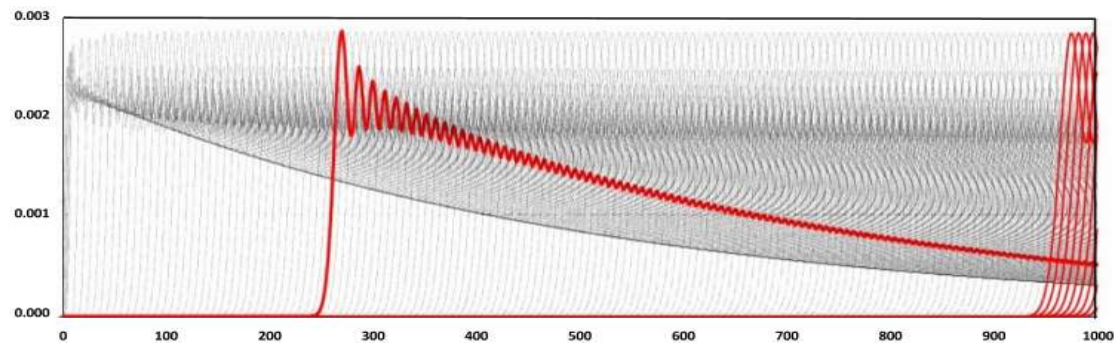

Fig. 8. Close-up of Fig. 8, near time axis
(0 ≤ τ ≤ 200). All functions θₙ are
represented, for 1 ≤ n ≤ 253, in gray,
**except θ₁, θ₄₃, θ₈₅, θ₁₂₇, θ₁₆₉, θ₂₁₁ and**
θ₂₅₃ which are in red.

In Fig. 9, 254 functions are represented to observe the shape of the same set of functions from $\tau = 0$ to $\tau = 1000$. They are designated in the legend. The function $\theta_{258}(\tau)$ is represented in red. This function is very close to the function $\theta_{253}(\tau)$ in Fig. 8. Therefore, it can be considered that it limits the set of functions already represented in Fig. 8. Those that are also in red, on the right side of the graph, show that for long time an almost periodic growth pattern has been established.

While $\theta_0(\tau)$ slowly decreases (Fig. 7) more and more very small layers are stacked on top of those that already exist, which are also very small. And the areas of solid support already covered grow much more in height than in width. They are like vertical fibbers that increase in length Therefore, in this example, the model can simulate a fibrillar biofilm.

Fig. 9. Close-up of Fig. 8, near time axis (0 ≤ τ ≤ 1000). Functions : θ_0, θ_1, θ_2, θ_3, θ_4, θ_5, θ_6 (θ_0 not visible) ... and θ_{13}, θ_{20}, θ_{27}, ... θ_{13+7n}, ... θ_{1203}, θ_{1210}, θ_{1218}, ... $\theta_{1210+8n}$, ... θ_{1810} and θ_{1818} (only visible till ≈ θ_{1014}). All the functions are represented in gray, except θ_{258}, θ_{958}, θ_{965}, θ_{972}, θ_{979}, θ_{986} θ_{993}, θ_{1000}, θ_{1007} and θ_{1014}, which are in red.

Fig. 10 is a close-up taken from Fig. 9 and provides a visualization of the growth pattern before fibrillar growth is reached. Fig. 11 is also a close-up made from Fig. 9 and provides a visualization of the growth pattern of the fibbers, almost only in height. The $\theta_n(\tau)$ functions of this example (Fig. 8 to 11) have an oscillating behaviour. Although positive, the values of the functions with this oscillating behaviour are very small. This detail can be observed due to the performed accuracy and is not surprising in systems with nonlinear dynamics, such this one.
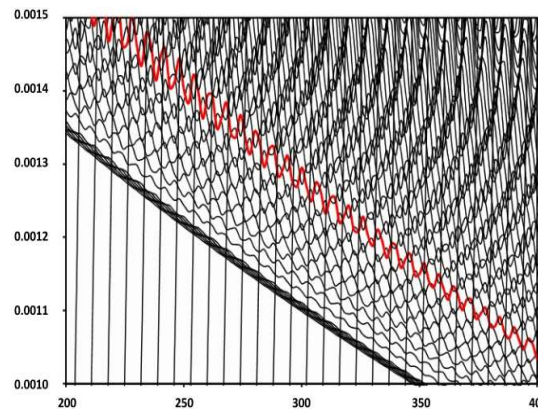
Fig. 10. Close-up of Fig. 10, near time axis. (200 ≤ τ ≤ 400).
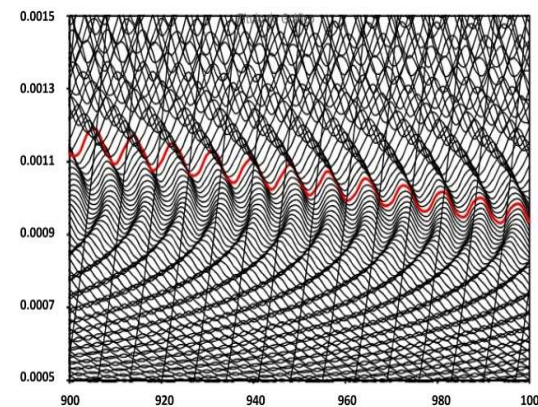
Fig. 11. Close-up of Fig. 10, near time axis. (900 ≤ τ ≤ 1000).

In Fig. 12 ($\phi = 0$ and $\delta = 1.5$) the entire specific rate growth is carried out in parallel to the solid support and the detachment is strong. It is observed that the system tends, in the cases of $\rho = 0.001, 0.01, 0.1$ and 0.2, to a well-defined steady state, in which the fraction of area not covered, $\theta_0(\tau)$, is much greater than all the others. In these cases the process of arrival and attachment and the growth parallel to the solid support don´t compensate the strong desorption. Therefore, the biofilm is patchy and consists only of small "hills" or clusters with one layer, two overlapping layers and little else.
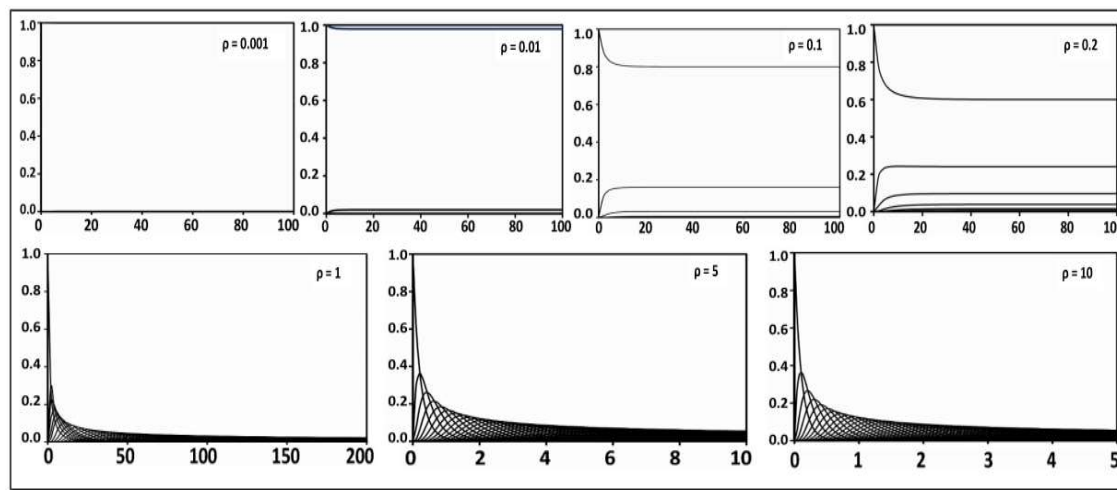

Fig. 12. θ$_n$(τ) functions for φ = 0 and δ = 1,5.

The close-ups of Fig. 13 show that $\theta_1(\tau), \theta_2(\tau)$ and following functions have also reached steady state. This was already observed in Fig. 12 for $\rho = 0.1$ (θ_1 and θ_2) and $\rho = 0.2$ (θ_1, θ_2 and θ_3).
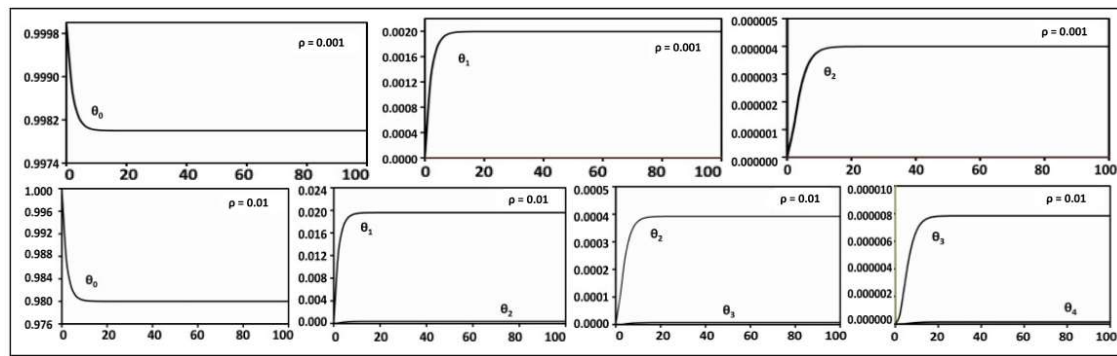

Fig. 13. Close-up of the plots in Fig. 7, near time axis and θ$_n$(τ) = 1 axis, for ρ = 0.001 and ρ = 0.01.

Table 3. (φ = 0; δ = 1.5) - (Refers to Fig. 12 and 13)	
ρ	Some values of θ$_n$(τ)
0.001	θ$_0$(100) = 0.998000000000 , θ$_1$(100) = 0.001996000000, θ$_2$(100) = 0.000003992000
0.01	θ$_0$(100) = 0.980000000000, θ$_1$(100) = 0.019600000000, θ$_2$(100) = 0.000392000000, θ$_3$(100) = 0.000000007984
0.1	θ$_0$(100) = 0.800000000367, θ$_1$(100) = 0.159999999950, θ$_2$(100) = 0.0319999998842797 , θ$_3$(100) = 0.006399999910
0.2	θ$_0$(100) = 0.600004540488, θ$_1$(100) = 0.240001080936, θ$_2$(100) = 0.095999524306,

		$\theta_3(100) = 0.038398981896$, $\theta_4(100) = 0.015358932530$
1		$\theta_0(200) = 0.000000000064$, $\theta_{101}(200) = 0.023261305240$ (θ_{101} is the maximum for $\tau = 200$)
5		$\theta_0(10) = 0.000000000001$, $\theta_{45}(10) = 0.053986479374$ (θ_{45} is the maximum for $\tau = 10$)
10		$\theta_0(5) \approx 0.000000000000$, $\theta_{47}(5) = 0.055197818334$ (θ_{47} is the maximum for $\tau = 5$)

In cases with $\rho = 1, 5$ and 10 the process of arrival and attachment is much more strong. Consequently $\theta_0(\tau)$ evolves to significantly smaller values. In this examples also an almost periodic growth pattern is established. The fractions covered with fewer layers are virtually zero and the fractions of greater thickness continue to grow, then reach a maximum and finally decrease because new layers grow over them. Biomass grows linearly over time due to this almost periodic evolution pattern.

The biofilm covers the entire solid support area, with an external interface on which the statistical distribution of thicknesses will remain unchanged in shape but whose average value increases with time. Therefore, the model builds a travelling wave front based on the microscopic description of the processes on which it is based. The histogram in Fig. 14 is this statistical distribution for $\rho = 10$ and $\tau = 5$. The biggest function is $\theta_{47}(\tau)$. Before $\tau = 5$ the maximum will have been a function $\theta_n(\tau)$ where $n < 47$. And for $\tau > 5$ the maximum will be a function $\theta_n(\tau)$ where $n > 47$.

The graph on the right side of Fig. 14 shows the functions $\theta_{35}(\tau)$, decreasing, $\theta_{47}(\tau)$, approximately constant at maximum and $\theta_{52}(\tau)$, growing. Then $\theta_{35}(\tau)$ will approach zero, $\theta_{47}(\tau)$ will decrease and $\theta_{52}(\tau)$ will reach its maximum, and so on. The increase in the order of functions means that the covered fractions have more and more layers of bacteria overlapping and therefore the total biomass increases. The global biomass increase which is equivalent of a mono layer that covers the entire solid support takes approximately the time of a period of the mentioned (almost) periodic evolution pattern.
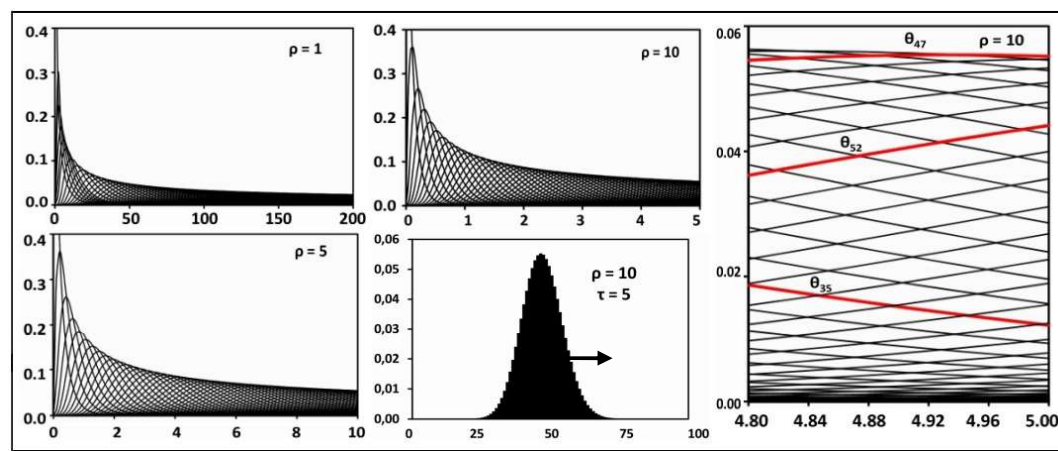

Fig. 14. Close-up of the plots in Fig. 7, for ρ = 1, 5 and 10, and histogram for ρ = 10 and τ = 5

Part V

9. Conclusions

A theoretical model of formation and growth of biofilms was described and its analytical solution was deduced for the more simplified version: only bacteria from the outermost layer are active and reproduce (L = 1). This solution has three components: one with Bessel functions of first kind (Case 1), one with Modified

Bessel functions of first kind (Case 2) and the borderline solution (Case 3). A recurring algorithm with five terms was built, whose accuracy allows calculations with 12 significant decimal places.

In Case 1, the function $\theta_0(\tau)$ has a root corresponding to the instant when the total coverage of the solid support is reached. It is because full coverage is achieved that it is called continuous biofilm. This happens in all the examples in Fig. 5 and those in Fig. 6 for $\rho \geq 0.1$. In Fig. 5, the local thicknesses obtained when the total coverage is reached vary from a single mono layer ($\rho = 0.001$) to a thickness distribution between 3 and 7 overlapping layers, with 5 being the thickness corresponding to the largest covered area.

In Fig. 6, for $\rho \geq 0.1$, the statistical thickness distributions represent higher values: from an average of approximately 100 overlapping layers ($\rho = 0.1$) to 10 ($\rho = 10$). Therefore, the structures in Fig. 5 and those in Fig. 6 for $\rho \geq 0.1$ vary between the monolayer and a wide variety of local thicknesses that give the outer interface of the biofilm a very irregular shape, with "deep valleys" and "high mountains". However, the time to fully cover the solid support varies greatly, depending on the choice of parameters ρ, ϕ and δ. Its duration can be so long that a pattern of almost periodic growth can be established before the solid support is completely covered. Is what happens in Fig. 6 for $\rho = 0.001$ and 0.01. As full coverage is achieved only after a long time, we can designate this biofilm as a pseudo patchy biofilm, so as not to confuse it with those in Case 2. In these cases, $\theta_0(\tau)$ remains positive, decreasing slowly.

For $\rho = 0.001$ a fibrillar biofilm structure is obtained (already described) and the fibers reach, for $\tau = 1000$, a height distribution centered in the interval between approximately 650 and 1000 overlapping layers. For $\rho = 0.01$ the uncovered fraction $\theta_0(\tau)$ is so small that the fibers occupy almost the entire solid support area. In this case, for $\tau = 1000$, the fibers have a height distribution centered in the interval between approximately 850 and 1020 overlapping layers.

An almost periodic growth pattern of $\theta_n(\tau)$ functions corresponds to a linear increase, over time, of total biomass. Is what happens in these two examples.

In Fig. 12 and 13 the model, with the solution of Modified Bessel functions of 1st kind, describes an evolution to a steady state for $\rho = 0.001, 0.01, 0.1$ and 0.2. This patchy biofilm consists only of small "hills" or clusters with one layer, two overlapping layers and little else.

For $\rho = 1, 5$ and 10 the model describes, once again, an almost periodic growth, with the corresponding linear increase in biomass. The biofilm covers the entire solid support and its outer interface is irregular, showing a statistical distribution of thicknesses whose shape remains but whose average moves, over time, to higher values. In this case the model is able to translate a traveling wave front into mathematical terms.

We can conclude that, even in its simplest version, the deduced model manages to simulate a wide variety of structures and, additionally, for certain parameter choices, it also goes beyond the initial phase of formation and growth, passing to the phase of total biomass linear growth, over time.

10. Future work

We can now relate some following deductions that can be done next.

The mathematical description of the linear phase of global biomass growth and accumulation can also be described for continuous biofilm (Case 1).

Once the already described process is started, at $\tau = 0$, there will come a time τ_1 when the fraction without any layer of bacteria θ_0 will cancel out: $\theta_0(\tau_1) = 0$. After this instant the solution remains mathematically correct but will not be physically meaningful   because θ_0 will pass, due to the continuity of the analytical

solution, to be negative and there are no surfaces whose area has a negative value. In the sequel we designate this solution, valid for $0 \leq \tau \leq \tau_1$ as "Solution 1".

Consequently, the following instants should no longer be calculated with this solution. But the values of the fractions θ_j, with $j \geq 1$, obtained at τ_1 will be the set of initial (positive) values of a new period of time, τ_2. Of course, the sum of these new initial values is 1.

In this new time interval τ_2 a more general analytical solution can be deduced and applied. Now we have several variables θ_j whose initial value must be taken into account and not just one. This more general analytical solution guarantees us the analytical continuity in of the model, solving the interval τ_2. In the sequel we designate this solution as "Solution 1*" and briefly describe this analytical continuation of the model.

During this second time interval, τ_2, it will now be the fraction θ_1 that will be annulled. When this happens, by the very same reason that there are no surfaces with negative area, we will again consider that the values θ_j, $j \geq 2$, obtained when $\theta_1(\tau_2) = 0$, will be the initial values of a third interval, τ_3. This third interval, ends when $\theta_2(\tau_3) = 0$. And so on: whenever the fraction θ_j, with the lowest index j (the smallest thickness fraction) cancels out, the following instants should no longer be calculated with the same exact solution since that fraction ceases to exist. Then at that instant, when θ_j, with the lowest index j cancels, the values (all positive) of all remaining fractions θ_j, will be the set of the initial values for a new time period.

Now we can summarize, in greater detail, the sequence of these successive solutions.

- Initial condition for interval 1 (lasting the time τ_1 and during which θ_0 will be canceled)
$$\theta_0(0) = 1, and\ \theta_j(0) = 0\ (for\ j \geq 1)$$
- Values at the end of interval 1 (obtained with "Solution 1")
$$\theta_0(\tau_1) = 0, and\ \theta_j(\tau_1) > 0\ (for\ j \geq 1)$$
- Initial condition for interval 2 (lasting the time τ_2 and during which θ_1 will be canceled)
$$\theta_j(0) = \theta_j(\tau_1), (for\ j \geq 1)$$
- Values at the end of interval 2 (obtained with "Solution 1*")
$$\theta_1(\tau_2) = 0, and\ \theta_j(\tau_2) > 0\ (for\ j \geq 2)$$
- Initial condition for interval 3 (lasting the time τ_3 and during which θ_2 will be canceled)
$$\theta_j(0) = \theta_j(\tau_2), (for\ j \geq 2)$$

... ...

- Values at the end of interval k-1 (obtained with "Solution 1*")
$$\theta_{k-2}(\tau_{k-1}) = 0, and\ \theta_j(\tau_{k-1}) > 0\ (for\ j \geq k - 1)$$
- Initial condition for interval k (lasting the time τ_k and during which θ_{k-1} will be canceled)
$$\theta_j(0) = \theta_j(\tau_{k-1}), (for\ j \geq k - 1)$$
- Values at the end of interval k (obtained with "Solution 1*")
$$\theta_{k-1}(\tau_k) = 0, and\ \theta_j(\tau_k) > 0\ (for\ j \geq k)$$

... ...

<u>Note:</u> When $k \to \infty$, $\tau_k \to \tau^*(\tau^*$ is constant) and $\theta_{j+1}(\tau_k) \to \theta_j(\tau_{k-1})$.

That is to say, the successive intervals of order k seem more and more to each other. The statistical distribution of the fractions θ_j tends to a histogram that, with the proviso that it suffers small variations between the beginning and the end of each interval, remains always the same. This histogram only shifts, over time, to θ_j with increasing indexes "j", increasing all of the "j" one unit for each "k"- interval elapsed. This is how the mathematical translation of a travelling front can be done for continuous biofilm (Case 1).

This "Solution 1*" is always the same for all intervals k (with $k \geq 1$) because all the fractions θ_j, at the beginning of the interval, have at least one layer of bacteria and this implies that all have growth potential by reproduction , and consequently the global population increases all over the entire surface. This does not happen in the first interval because, during this interval, there is θ_0, with a non-zero value ($\theta_0 > 0$). Mathematically this "Solution 1*" is always the same because it starts from a system of differential-difference equations in which the first one explicitly expresses the derivative of θ_{k-1} following those of θ_k, θ_{k+1}, ... changing only the interval order k. This does not influence the deduction that leads to the successive solutions. It is only necessary to properly replace the index k as well as the initial conditions that correspond to it.

"Solution 1", applicable only to the first interval, is therefore not exactly just a particular case of "Solution 1*" although this one may be used with any initial condition that we consider convenient. This is so because there are details that distinguish the equation for the derivative of θ_0 from the equation of the derivative of θ_{k-1} , for all other intervals, when one put $k = 1$ in this last equation.

The deduction just explained will be next work.

Another future development can be the determination of total biomass evolution over time and also of several variables that characterize the structure.

A mono-layer sufficient to cover the surface unit of the solid support is the biomass unit.

With the evolution over time of all the factions $\theta_i(\tau)$, the evolution over time of the total biomass can be easily calculated,

$$Biofilm\ biomass = \sum_{i=0}^{\infty} i \cdot \theta_i(\tau)$$

And also, several structural variables:

The areal porosity,

$$Areal\ porosity\ at\ the\ level\ of\ the\ first\ layer = \theta_0(\tau),$$
$$Areal\ porosity\ at\ the\ level\ of\ the\ second\ layer = \theta_0(\tau) + \theta_1(\tau)$$
$$\ldots\ldots\ldots\ldots\ldots\ldots\ldots\ldots\ldots\ldots\ldots\ldots\ldots\ldots\ldots\ldots\ldots\ldots\ldots\ldots\ldots\ldots$$

$$Areal\ porosity\ at\ the\ level\ of\ the\ nth\ layer = \sum_{i=0}^{n-1} \theta_i(\tau)$$

The biofilm porosity,

$$Biofilm\ porosity = 1 - \frac{1}{N} \cdot \sum_{i=0}^{N} i \cdot \theta_i(\tau),$$

where N is the maximum thickness of all functions $\theta_i(\tau)$ that have a non $-$ negligible value .

And the structural entropy,

$$Structural\ entropy = \frac{1}{N+1} \cdot \sum_{i=0}^{N} \theta_i(\tau) \cdot log\ \theta_i(\tau)$$

... where if one $\theta_i(\tau)$ is zero, the term in the sum is zero.

The greater the structural entropy, the more irregular is the biofilm is and, therefore, the greater the variety of local thicknesses.

All these parameters are also an immediate result of the application of the model and will be the object of future computation and analysis.

Appendix A. Continuous biofilm solution

Now follows the solution for continuous biofilm, (Case 1).

Lets recall the equation given earlier as eq. (71),

$$g(s,\tau) = \frac{e^{-(\rho+\Phi)\cdot(1-\Phi-\delta)\cdot\frac{\tau}{s}}}{s} + \int_0^\tau f(\sigma) \cdot \frac{e^{-(\rho+\Phi)\cdot(1-\Phi-\delta)\cdot\frac{(\tau-\sigma)}{s}}}{s} \cdot d\sigma$$

Applying inverse Laplace transform we get,

$$G(z,\tau) = J_0\left(2\cdot\sqrt{(\rho+\Phi)\cdot(1-\Phi-\delta)\cdot\tau\cdot z}\right) + \cdot$$

$$+ \int_0^\tau J_0\left(2\cdot\sqrt{(\rho+\Phi)\cdot(1-\Phi-\delta)\cdot(\tau-\sigma)\cdot z}\right)\cdot f(\sigma)\cdot d\sigma \qquad (A1)$$

At this point, it is convenient to define other functions, related to Bessel functions, but easier for calculation purposes. We will need to derive partially relatively to τ and z when the conditions in generating function formalism, before established, must be satisfied. However such derivations applied directly in Bessel functions are somewhat cumbersome. Such more adequate functions are,

$$V_n(\sigma,\tau,z) = \left[\frac{(\tau-\sigma)}{(\rho+\Phi)\cdot(1-\Phi-\delta)\cdot z}\right]^{n/2} \cdot J_n\left(2\cdot\sqrt{(\rho+\Phi)\cdot(1-\Phi-\delta)\cdot(\tau-\sigma)\cdot z}\right) \qquad (A2)$$

Their derivatives are very simple to use, according to the following rules,

$$\frac{\partial V_n(\sigma,\tau,z)}{\partial z} = -(\rho+\Phi)\cdot(1-\Phi-\delta)\cdot V_{n+1}(\sigma,\tau,z)$$

$$(A3)$$

$$\frac{\partial V_n(\sigma,\tau,z)}{\partial \tau} = V_{n-1}(\sigma,\tau,z)$$

$$(A4)$$

Demonstration of these rules are long and tedious. So we will pursue simply accepting them. Inserting (A2) in (A1),

$$G(z,\tau) = V_0(0,\tau,z) + \int_0^\tau V_0(\sigma,\tau,z)\cdot f(\sigma)\cdot d\sigma$$

$$(A5)$$

Now this solution must satisfy the early designated condition (58), which has not yet been taken in consideration. For achieve that goal we must determine function $f(\sigma)$. Let define $f(\sigma)$ by an infinite power series,

$$f(\sigma) = \sum_{k=0}^\infty c_k \cdot \sigma^k \qquad (A6)$$

... and include the power series in (A5),

$$G(z,\tau) = V_0(0,\tau,z) + \sum_{k=0}^\infty c_k \cdot \left[\int_0^\tau V_0(\sigma,\tau,z)\cdot \sigma^k \cdot d\sigma\right] \qquad (A7)$$

The integrals,

$$\int_0^\tau V_0(\sigma,\tau,z) \cdot \sigma^k \cdot d\sigma$$

... can be calculated introducing the definition of the function $V_0(\sigma,\tau,z)$ and applying the identity,

$$\int_0^\tau (\tau - \sigma)^i \cdot \sigma^k \cdot d\sigma = \frac{k!\,i!}{(k+i+1)!} \cdot \tau^{k+i+1} \tag{A8}$$

The result, which we here only indicate, is,

$$\int_0^\tau V_0(\sigma,\tau,z) \cdot \sigma^k \cdot d\sigma = k! \cdot V_{k+1}(0,\tau,z) \tag{A9}$$

The consequent sequel is that (A7) becomes,

$$G(z,\tau) = V_0(0,\tau,z) + \sum_{k=0}^\infty c_k \cdot k! \cdot V_{k+1}(0,\tau,z) \tag{A10}$$

Rules (A3) and (A4) came now into play to accomplish already defined condition (58) in this last equation. Calculating the partial derivatives of the generating function in (A10) they reads,

$$\frac{\partial G(z,\tau)}{\partial \tau} = V_{-1}(0,\tau,z) + \sum_{k=0}^\infty c_k \cdot k! \cdot V_k(0,\tau,z) \tag{A11}$$

$$\frac{\partial G(z,\tau)}{\partial z} = -(\rho + \Phi) \cdot (1 - \Phi - \delta) \cdot \left[V_1(0,\tau,z) + \sum_{k=0}^\infty c_k \cdot k! \cdot V_{k+2}(0,\tau,z) \right] \tag{A12}$$

Easily one can prove,

$$V_{-n}(\sigma,\tau,z) = \left[\frac{(-1)(\rho + \Phi)(1 - \Phi - \delta)}{(\tau - \sigma)} \right]^n \cdot V_n(\sigma,\tau,z) \tag{A13}$$

Formula (A13) avoids the utilization of functions of negative order. It can be used straightaway in (A11),

$$\frac{\partial G(z,\tau)}{\partial \tau} = -\frac{(\rho + \Phi) \cdot (1 - \Phi - \delta) \cdot z}{\tau} \cdot V_1(0,\tau,z) + \sum_{k=0}^\infty c_k \cdot k! \cdot V_k(0,\tau,z) \tag{A14}$$

At last the two partial derivatives of the generating function at $z = \tau$ can be written,

$$\left[\frac{\partial G(z,\tau)}{\partial \tau} \right]_{z=\tau} = -(\rho + \Phi) \cdot (1 - \Phi - \delta) \cdot V_1(0,\tau,\tau) + \sum_{k=0}^\infty c_k \cdot k! \cdot V_k(0,\tau,\tau) \tag{A15}$$

$$\left[\frac{\partial G(z,\tau)}{\partial z} \right]_{z=\tau} = -(\rho + \Phi) \cdot (1 - \Phi - \delta) \cdot \left[V_1(0,\tau,\tau) + \sum_{k=0}^\infty c_k \cdot k! \cdot V_{k+2}(0,\tau,\tau) \right] \tag{A16}$$

The left hand side of early condition (58) is (A15), and is now possible to write it putting the functions $V_k(0,\tau,\tau)$ in increasing order n,

$$\left[\frac{\partial G(z,\tau)}{\partial \tau} \right]_{z=\tau} = c_0 \cdot V_0(0,\tau,\tau) + [c_1 - (\rho + \Phi) \cdot (1 - \Phi - \delta)] \cdot V_1(0,\tau,\tau) + \sum_{k=2}^\infty c_k \cdot k! \cdot V_k(0,\tau,\tau) \tag{A17}$$

In the same way, the right hand side of (58) can be rewritten substituting there (A10) and (A16). And also with the functions $V_k(0,\tau,\tau)$ in increasing order n,

$$(2 \cdot \Phi + \delta - 1) \cdot G(\tau, \tau) - \frac{\Phi}{(\rho + \Phi)} \cdot \left(\frac{\partial G}{\partial z}\right)_{z=\tau} =$$

$$= (2 \cdot \Phi + \delta - 1) \cdot V_0(0, \tau, \tau) + [(2 \cdot \Phi + \delta - 1) \cdot c_0 - \Phi \cdot (1 - \Phi - \delta)] \cdot V_1(0, \tau, \tau) +$$

$$+ \sum_{k=0}^{\infty} [\Phi \cdot (1 - \Phi - \delta) \cdot c_k \cdot k! + (2 \cdot \Phi + \delta - 1) \cdot c_{k+1} \cdot (k+1)!] \cdot V_{k+2}(0, \tau, \tau) \quad (A18)$$

Early obtained equation (58) implies to equalize the right hand sides of (A17) and (A18). Such equalization only will be valid if the factors affecting each function $V_k(0, \tau, \tau)$ are equal on those both right hand sides. In this way a system of algebraic equations is established and, from that system, all the coefficients c_k defined without ambiguity. And, at last, the generating function is completely defined. The aforesaid system, extracted from (A17) and (A18), is,

$$c_0 = (2 \cdot \Phi + \delta - 1) \qquad\qquad (A19 \, (0))$$

$$c_1 - (\rho + \Phi) \cdot (1 - \Phi - \delta) = \Phi \cdot (1 - \Phi - \delta) + (2 \cdot \Phi + \delta - 1) \cdot c_0 \qquad\qquad (A19 \, (1))$$

$$c_2 \cdot 2! = \Phi \cdot (1 - \Phi - \delta) \cdot c_0 + (2 \cdot \Phi + \delta - 1) \cdot c_1 \qquad\qquad (A19 \, (2))$$

$$c_3 \cdot 3! = \Phi \cdot (1 - \Phi - \delta) \cdot c_1 + (2 \cdot \Phi + \delta - 1) \cdot c_2 \cdot 2! \qquad\qquad (A19 \, (3))$$

$$c_4 \cdot 4! = \Phi \cdot (1 - \Phi - \delta) \cdot c_2 \cdot 2! + (2 \cdot \Phi + \delta - 1) \cdot c_3 \cdot 3! \qquad\qquad (A19 \, (4))$$

$- -$

$$c_{k+2} \cdot (k+2)! = \Phi \cdot (1 - \Phi - \delta) \cdot c_k \cdot k! + (2 \cdot \Phi + \delta - 1) \cdot c_{k+1} \cdot (k+1)! \qquad (A19 \, (k+2))$$

$- -$

The two first (A19 (0)) and (A19 (1)) are preliminary conditions and all the others have the general form given by (A19 (k+2)). This last one is a difference equation which form can be also put like,

$$b_{k+2} + A \cdot b_{k+1} + B \cdot b_k = 0 \qquad\qquad (A20)$$

… where,

$$b_k = c_k \cdot k! \qquad\qquad (A21)$$

$$A = (1 - 2 \cdot \Phi - \delta) \qquad\qquad (A22)$$

$$B = \Phi \cdot (\Phi + \delta - 1) \qquad\qquad (A23)$$

The general solution of (A20) is known elsewhere,

$$b_k = \frac{[b_1 + b_0(A + r_1)]}{(r_1 - r_2)} \cdot r_1^k - \frac{[b_1 + b_0(A + r_2)]}{(r_1 - r_2)} \cdot r_2^k \qquad\qquad (A24)$$

… where the roots are,

$$r_1 = \frac{-A + \sqrt{A^2 - 4 \cdot B}}{2} \qquad\qquad r_2 = \frac{-A - \sqrt{A^2 - 4 \cdot B}}{2} \qquad\qquad (A25)$$

In the case under analysis, inserting (A22) and (A23) in (A25),

$$r_1 = \Phi \qquad\qquad r_2 = (\Phi + \delta - 1) \qquad\qquad (A26)$$

Substitution in (A24) and consideration of (A21) leads to the coefficients c_k,

$$c_k \cdot k! = \frac{1}{(1 - \delta)} \cdot \{[c_1 + c_0 \cdot (1 - \Phi - \delta)] \cdot \Phi^k - (c_1 - c_0 \cdot \Phi) \cdot (\Phi + \delta - 1)^k\} \qquad (A27)$$

The coefficient c_0 is given by (A19 (0)) and c_1 can be obtained by (A19 (1)),

$$c_1 = (1 - \Phi - \delta) \cdot (\rho + 2 \cdot \Phi) + (2 \cdot \Phi + \delta - 1)^2 \qquad (A28)$$

Now c_0 and c_1 are eliminated from (A27) by substitution,

$$c_k = \frac{1}{(1-\delta) \cdot k!} \cdot \{[\rho \cdot (1 - \Phi - \delta) + \Phi \cdot (1 - \delta)] \cdot \Phi^k + (\rho + 1 - \delta) \cdot (\Phi + \delta - 1)^{k+1}\} \qquad (A29)$$

Formula (A29) is valid for $k \geq 1$. For $k = 0$, the formula (A19 (0)) must be used for calculate c_0. Considering (A21) we can use, from now on, the coefficients b_k or the c_k. For sake of economy in notation is better to chose, from now on, only the coefficients b_k.

What is achieved till now about these coefficients can be appropriately summarized,

$$b_k = \begin{cases} (2 \cdot \Phi + \delta - 1) \dots for\ k = 0 & (A30\ (0)) \\[2em] \dfrac{\{[\rho \cdot (1 - \Phi - \delta) + \Phi \cdot (1 - \delta)] \cdot \Phi^k + (\rho + 1 - \delta) \cdot (\Phi + \delta - 1)^{k+1}\}}{(1 - \delta)} \\[1em] \hfill \dots for\ k \geq 1 \quad (A30\ (k)) \end{cases}$$

Taking in consideration (A21) and substituting these two expressions in (A10) one gets the final wanted formula for the generating function,

$$G(z, \tau) = V_0(0, \tau, z) + (2 \cdot \Phi + \delta - 1) \cdot V_1(0, \tau, z) +$$

$$+ \frac{1}{(1-\delta)} \cdot \sum_{k=1}^{\infty} \{[\rho \cdot (1 - \Phi - \delta) + \Phi \cdot (1 - \delta)] \cdot \Phi^k + (\rho + 1 - \delta) \cdot (\Phi + \delta - 1)^{k+1}\} \cdot V_{k+1}(0, \tau, z)$$

$$(A31)$$

Functions $Q_n(\tau)$ are defined by the early eq. (60). But let first generalize (A3) for n derivations (is convenient change n by k in (A3) and then to derive n times),

$$\frac{\partial^n V_k(\sigma, \tau, z)}{\partial z^n} = (-1)^n \cdot [(\rho + \Phi) \cdot (1 - \Phi - \delta)]^n \cdot V_{k+n}(\sigma, \tau, z)$$

$$(A32)$$

Applying in (A31),

$$\frac{\partial^n G(z, \tau)}{\partial z^n} = (-1)^n \cdot [(\rho + \Phi) \cdot (1 - \Phi - \delta)]^n \cdot \left\{ V_n(0, \tau, z) + b_0 \cdot V_{n+1}(0, \tau, z) + \sum_{k=1}^{\infty} b_k \cdot V_{n+k+1}(0, \tau, z) \right\}$$

$$(A33)$$

Where b_0 and b_k are defined by $(A30\ (0))$ and $(A30\ (k))$.

Lastly, functions $Q_n(\tau)$, for $n \geq 1$, are,

$$Q_n(\tau) = -\frac{(-1)^n \cdot \rho}{(\rho + \Phi) \cdot (1 - \Phi - \delta)^n} \cdot \left(\frac{\partial^n G}{\partial z^n} \right)_{z=\tau} \dots \dots for\ (n \geq 1) \qquad (A34)$$

Resulting, for $n \geq 1$,

$$Q_n(\tau) = \rho \cdot (\rho + \Phi)^{n-1} \cdot \left\{ V_n(0, \tau, \tau) + b_0 \cdot V_{n+1}(0, \tau, \tau) + \sum_{k=1}^{\infty} b_k \cdot V_{n+k+1}(0, \tau, \tau) \right\}$$

$$(A35)$$

The fractions $\theta_n(\tau)$, for $n \geq 1$ are reached with the substitution, already named (28),

$$\theta_n(\tau) = e^{-(\rho + 2 \cdot \Phi - \delta - 1) \cdot \tau} \cdot Q_n(\tau) \tag{28}$$

The fraction $\theta_0(\tau)$ is obtained from (A30), putting $z = \tau$, because $Q_0(\tau) = G(\tau, \tau)$, and then also applying (28). The desired solution for Case 1, in terms of Bessel functions of first kind, $J_n(x)$, is eq. (80) which can now be found in section 6.2.

For such achievement one only need to apply the early defined formula (81), but inverting, so making explicit the functions $J_n\left(2 \cdot \sqrt{(\rho + \Phi) \cdot (1 - \Phi - \delta) \cdot (\tau - \sigma) \cdot z}\right)$,

$$J_n\left(2 \cdot \sqrt{(\rho + \Phi) \cdot (1 - \Phi - \delta) \cdot (\tau - \sigma) \cdot z}\right) = \left[\frac{(\rho + \Phi) \cdot (1 - \Phi - \delta) \cdot z}{(\tau - \sigma)}\right]^{n/2} \cdot V_n(\sigma, \tau, z) \tag{A36}$$

Appendix B. Patchy biofilm solution

Let recall that the solution (117) is only the solution for the named Case 1, corresponding to the continuous biofilm. As signalled before, (117) corresponds to the condition $\delta < (1 - \Phi)$.

The "complementary" condition, $\delta > (1 - \Phi)$, designated before as Case 2, relates the evolution towards a steady state where the bare fraction θ_0 don´t never get null. In physical terms this means the formation, at times large enough, of a patchy biofilm.

The solution for Case 2 can be obtained simply from solution (117), being aware that whenever root $\sqrt{1 - \Phi - \delta}$ occurs substitution by $i \cdot \sqrt{\Phi + \delta - 1}$ must be done. Consequently, in (117) the variable x and the coefficients α_n and β_k are modified as follows.

Variable x changes this way,

$$x = 2 \cdot \tau \cdot \sqrt{(\rho + \Phi) \cdot (1 - \Phi - \delta)}$$
$$2 \cdot \tau \cdot \sqrt{(\rho + \Phi) \cdot (1 - \Phi - \delta)} = i \cdot 2 \cdot \tau \cdot \sqrt{(\rho + \Phi) \cdot (\Phi + \delta - 1)}$$
$$i \cdot 2 \cdot \tau \cdot \sqrt{(\rho + \Phi) \cdot (\Phi + \delta - 1)} = i \cdot x^*$$

So the change in variable x reads,

$$x \to (i \cdot x^*) \tag{B1}$$

Coefficient α_n changes this way,

$$\frac{\rho \cdot (\rho + \Phi)^{n-1}}{\sqrt{(\rho + \Phi)^n \cdot (1 - \Phi - \delta)^n}} = \frac{\rho \cdot (\rho + \Phi)^{n-1}}{i^n \cdot \sqrt{(\rho + \Phi)^n \cdot (\Phi + \delta - 1)^n}}$$

$$\frac{\rho \cdot (\rho + \Phi)^{n-1}}{i^n \cdot \sqrt{(\rho + \Phi)^n \cdot (\Phi + \delta - 1)^n}} = i^{-n} \cdot a_n^*$$

So the change in coefficient α_n reads,

$$\alpha_n \to (i^{-n} \cdot a_n^*) \tag{B2}$$

And the new coefficient α_n^* is now, for all values of n,

$$\alpha_n^* = \begin{cases} 1 \ ... for \ n = 0 & (B3\,(0)) \\ \\ \dfrac{\rho \cdot (\rho + \Phi)^{n-1}}{\sqrt{(\rho + \Phi)^n \cdot (\Phi + \delta - 1)^n}} ... only \ for \ n \geq 1 & (B3\,(k)) \end{cases}$$

Coefficient β_1 changes this way,

$$\beta_1 = \frac{(2 \cdot \Phi + \delta - 1)}{\sqrt{(\rho + \Phi) \cdot (1 - \Phi - \delta)}}$$

$$\frac{(2 \cdot \Phi + \delta - 1)}{\sqrt{(\rho + \Phi) \cdot (1 - \Phi - \delta)}} = \frac{(2 \cdot \Phi + \delta - 1)}{i \cdot \sqrt{(\rho + \Phi) \cdot (\Phi + \delta - 1)}}$$

$$\frac{(2 \cdot \Phi + \delta - 1)}{i \cdot \sqrt{(\rho + \Phi) \cdot (\Phi + \delta - 1)}} = i^{-1} \cdot \beta_1^*$$

So the change in coefficient β_1 reads,

$$\beta_1 \to (i^{-1} \cdot \beta_1^*) \tag{B4}$$

Coefficient β_k, for $(k \geq 2)$, changes this way,

$$\beta_k = \frac{\{[\rho \cdot (1 - \Phi - \delta) + \Phi \cdot (1 - \delta)] \cdot \Phi^{k-1} + (\rho + 1 - \delta) \cdot (\Phi + \delta - 1)^k\}}{(1 - \delta) \cdot \sqrt{(\rho + \Phi)^k \cdot (1 - \Phi - \delta)^k}}$$

... but the numerator can be written using the b_k definition,

$$b_{k-1} = \{[\rho \cdot (1 - \Phi - \delta) + \Phi \cdot (1 - \delta)] \cdot \Phi^{k-1} + (\rho + 1 - \delta) \cdot (\Phi + \delta - 1)^k\}$$

(observe that in the numerator b_{k-1} doesn´t exist any square root, so it remains the same)

... thus lightning the notation,

$$\beta_k = \frac{b_{k-1}}{\sqrt{(\rho + \Phi)^k \cdot (1 - \Phi - \delta)^k}}$$

$$\frac{b_{k-1}}{\sqrt{(\rho + \Phi)^k \cdot (1 - \Phi - \delta)^k}} = \frac{b_{k-1}}{i^k \cdot \sqrt{(\rho + \Phi)^k \cdot (\Phi + \delta - 1)^k}}$$

$$\frac{b_{k-1}}{i^k \cdot \sqrt{(\rho + \Phi)^k \cdot (\Phi + \delta - 1)^k}} = i^{-k} \cdot \beta_k^*$$

So the change in coefficient β_k, wherever occurs, reads,

$$\beta_k \to (i^{-k} \cdot \beta_k^*) \tag{B5}$$

And the new coefficient β_k^* is now, for all values of n,

$$\beta_0^* = 1 \tag{B6 (0)}$$

$$\beta_1^* = \frac{(2 \cdot \Phi + \delta - 1)}{\sqrt{(\rho + \Phi) \cdot (\Phi + \delta - 1)}} \tag{B6 (1)}$$

$$\beta_k^* = \frac{\{[\rho \cdot (1 - \Phi - \delta) + \Phi \cdot (1 - \delta)] \cdot \Phi^{k-1} + (\rho + 1 - \delta) \cdot (\Phi + \delta - 1)^k\}}{(1 - \delta) \cdot \sqrt{(\rho + \Phi)^k \cdot (\Phi + \delta - 1)^k}}$$

$$... only\ for\ k \geq 2 \tag{B6 (k)}$$

Lastly and easily the solution for Case 2 (patchy biofilm) can now be written taking the early deduced in Appendix A, eq.(80) as starting point, and applying the preceding obtained changes in coefficients.

Step by step:

$$\theta_n(\tau) = \alpha_n \cdot e^y \cdot \sum_{k=0}^{\infty} \beta_k \cdot J_{n+k}(x) \tag{80}$$

Using $(B1), (B2)$ and $(B5)$,

$$\alpha_n \cdot e^y \cdot \sum_{k=0}^{\infty} \beta_k \cdot J_{n+k}(x) = i^{-n} \cdot a_n^* \cdot e^y \cdot \sum_{k=0}^{\infty} i^{-k} \cdot \beta_k^* \cdot J_{n+k}(i \cdot x^*) \tag{B7}$$

Recalling that $J_n(i \cdot x) = i^n \cdot I_n(x)$,

$$i^{-n} \cdot a_n^* \cdot e^y \cdot \sum_{k=0}^{\infty} i^{-k} \cdot \beta_k^* \cdot J_{n+k}(i \cdot x^*) = i^{-n} \cdot a_n^* \cdot e^y \cdot \sum_{k=0}^{\infty} i^{-k} \cdot \beta_k^* \cdot i^{n+k} \cdot I_{n+k}(x^*) \tag{B8}$$

Associating all the factors i^{-n}, i^{-k} and i^{n+k},

$$i^{-n} \cdot a_n^* \cdot e^y \cdot \sum_{k=0}^{\infty} i^{-k} \cdot \beta_k^* \cdot i^{n+k} \cdot I_{n+k}(x^*) = a_n^* \cdot e^y \cdot \sum_{k=0}^{\infty} \beta_k^* \cdot I_{n+k}(x^*) \tag{B9}$$

Finally, concatenating the already obtained eq. (80) with $(B7)$, then with $(B8)$ and lastly with $(B9)$ the searched solution reads,

$$\theta_n(\tau) = a_n^* \cdot e^y \cdot \sum_{k=0}^{\infty} \beta_k^* \cdot I_{n+k}(x^*) \tag{B10}$$

This is eq. (81) and represents the solution for case 2 (Patchy biofilm). Can now be found completely written down in section 6.2.

Appendix C. Frontier between continuous and patchy biofilm solution

The solution for Case 3 can be easily deduced by induction after doing the corresponding simplifications in the initial system of differential-difference master equations, just before any other step. It is so simple that we only indicate the solution,

$$\theta_0(\tau) = e^{-\rho\tau} \tag{C1(0)}$$

$$\theta_n(\tau) = e^{-(\rho+\Phi)\cdot\tau} \cdot \frac{\rho \cdot (\rho + \Phi)^{n-1}}{\Phi^n} \left\{ e^{\Phi\tau} - \sum_{k=0}^{n-1} \frac{(\tau \cdot \Phi)^k}{k!} \right\} \qquad \dots for \ (n>0) \tag{C1 (n)}$$

This solution is coherent with earlier found solution (80) for Case 1 and it is important and interesting to check that coherence. We can achieve that goal written solution eq. (80) in this alternative form,

Solution for case 1: continuous biofilm $[\delta<(1-\Phi)]$ (alternative representation)

$$\theta_n(\tau) = A_n \cdot e^y \cdot \sum_{k=0}^{\infty} B_k \cdot \frac{J_{n+k}(x)}{\gamma^{n+k}} \tag{C2}$$

Where:

$x = 2 \cdot \tau \cdot \gamma$

$y = (1 - \rho - 2 \cdot \Phi - \delta) \cdot \tau$

$\gamma = \sqrt{(\rho + \Phi) \cdot (1 - \Phi - \delta)}$

$A_0 = 1$

$A_n = \rho \cdot (\rho + \Phi)^{n-1} \dots only \ for \ n \geq 1$

$B_0 = 1$

$B_1 = (2 \cdot \Phi + \delta - 1)$

$B_k = \dfrac{\{[\rho \cdot (1 - \Phi - \delta) + \Phi \cdot (1 - \delta)] \cdot \Phi^{k-1} + (\rho + 1 - \delta) \cdot (\Phi + \delta - 1)^k\}}{(1 - \delta)} \qquad \dots only \ for \ k \geq 2$

When $\delta = 1 - \Phi$, $\gamma = 0$ and, in the summation in $(C2)$, each Bessel function term assumes the following value,

$$\frac{J_{n+k}(x)}{\gamma^{n+k}} = \frac{1}{\gamma^{n+k}} \cdot \sum_{i=0}^{\infty} \frac{(-1)^i \cdot (\tau \cdot \gamma)^{n+k+2 \cdot i}}{i! \cdot (n + k + i)!}$$

$$\frac{1}{\gamma^{n+k}} \cdot \sum_{i=0}^{\infty} \frac{(-1)^i \cdot (\tau \cdot \gamma)^{n+k+2 \cdot i}}{i! \cdot (n + k + i)!} = \sum_{i=0}^{\infty} \frac{(-1)^i \cdot \tau^{n+k+2 \cdot i} \cdot \gamma^{2 \cdot i}}{i! \cdot (n + k + i)!}$$

Consequently, if $\gamma = 0$,

$$\frac{J_{n+k}(x)}{\gamma^{n+k}} = \frac{\tau^{n+k}}{(n + k)!}$$

And inserting in $(C2)$,

$$\theta_n(\tau) = A_n \cdot e^y \cdot \sum_{k=0}^{\infty} B_k \cdot \frac{\tau^{n+k}}{(n+k)!}$$

Coefficients B_k simplify,

$$B_k = \Phi^k \dots for \ (k \geq 0)$$

… as well as y,

$$y = -(\rho + \Phi) \cdot \tau$$

Now we conclude that,

$$\theta_0(\tau) = e^{-(\rho+\Phi)\cdot\tau} \cdot \sum_{k=0}^{\infty} \Phi^k \cdot \frac{\tau^k}{k!}$$

… and,

$$e^{-(\rho+\Phi)\cdot\tau} \cdot \sum_{k=0}^{\infty} \Phi^k \cdot \frac{\tau^k}{k!} = e^{-(\rho+\Phi)\cdot\tau} \cdot e^{\Phi\cdot\tau}$$

… and,

$$e^{-(\rho+\Phi)\cdot\tau} \cdot e^{\Phi\cdot\tau} = e^{-\rho\cdot\tau}$$

Concatenating those last three equalities one obtains $(C1(0))$,

And, when $(n \geq 1)$,

$$\theta_n(\tau) = \rho \cdot (\rho + \Phi)^{n-1} \cdot e^{-(\rho+\Phi)\cdot\tau} \cdot \sum_{k=0}^{\infty} \Phi^k \cdot \frac{\tau^{n+k}}{(n+k)!}$$

… and also,

$$\rho \cdot (\rho + \Phi)^{n-1} \cdot e^{-(\rho+\Phi)\cdot\tau} \cdot \sum_{k=0}^{\infty} \Phi^k \cdot \frac{\tau^{n+k}}{(n+k)!} = e^{-(\rho+\Phi)\cdot\tau} \cdot \frac{\rho \cdot (\rho + \Phi)^{n-1}}{\Phi^n} \cdot \sum_{k=0}^{\infty} \frac{(\Phi \cdot \tau)^{n+k}}{(n+k)!}$$

But, once the following identity, holds,

$$\sum_{k=0}^{\infty} \frac{(\Phi \cdot \tau)^{n+k}}{(n+k)!} = e^{-\rho\cdot\tau} - \sum_{k=0}^{n-1} \frac{(\Phi \cdot \tau)^k}{k!}$$

… we get,

$$\theta_n(\tau) = e^{-(\rho+\Phi)\cdot\tau} \cdot \frac{\rho \cdot (\rho + \Phi)^{n-1}}{\Phi^n} \left\{ e^{\Phi\tau} - \sum_{k=0}^{n-1} \frac{(\tau \cdot \Phi)^k}{k!} \right\} \dots for \ (n>0)$$

… which is equal to $(C1(n))$, as we wanted to demonstrate.

References

1. White J. A., Schmidt, J. W., and Bennett G. K., Analysis of Queueing Systems, Academic Press, New York (1975)
2. Kleinrock, L., Queueing Systems, vol.1: Theory, Wiley, New York (1975)

3. Akimaru,H., and Kawashima K., Teletraffic: Theory and Applications (2º ed), Springer, London (1999)

4. Yan, Houmin, Yin, George, Zhang, Qing, Eds., Stochastic Processes, Optimization, and Control Theory: Applications in Financial Engineering, Queueing Networks, and Manufacturing Systems, Springer (2006)

5. Abate, J., and Whitt W., Calculating Time-Dependent Performance Measures for the M/M/1 Queue. IEEE Transactions on Communications, vol. 37, No. 10, (1989), pp. 1102-1104

6. C.G. Cassandras and S. Lafortune, Introduction to Discrete Event Systems (2º edition), Springer, (2010)

7. Marvin K. Simon, Mohamed-Slim Alouini, Digital Communication over Fading Channels, 2nd Edition, Wiley-IEEE Press, (2005)

8. Thomas G. Robertazzi**,** Computer Networks and Systems: Queueyng Theory and Performance Evaluation, (3rd edition), Springer (2000)

9. Ryszard Syski, Introduction to congestion theory in telephone systems, 2ª edition, North-Holland, (1986)

10. Goodrich, F. C., Nucleation Rates and the Kinetics of Particle Growth. II. The Birth and Death Process, Proc.Roy.Soc.Lond. A 277 (1964) 167-182

11. Carvalho, J. M., From discrete biofilm model formation to queuing transient analysis, https://run.unl.pt/handle/10362/77252, Ph. D. thesis (Chemical and Biochemical Engineering), Nova University of Lisbon, Lisbon (2018)

12. Amparo Gil, Javier Segura and Nico M. Temme, Numerical Methods for Special Functions, SIAM, (2007)

13. H. C. Thacher, "New Backward Recurrences for Bessel Functions", Math. Comp., vol. 33, nº 146, 744-764, (1979)

14. Clarke A. B., A Waiting Line Process of Markov Type, The Annals of Mathematical Statistics, Vol. 27, No. 2 (Jun., 1956), pp. 452-459.

15. Pinney, E., Ordinary Difference-Differential Equations, University of California Press (1958)

16. Bellman, R., and Cooke, K.L., Differential-Difference Equations, Academic Press (1963)

17. El'sgol'ts, L.E. e Norkin,S.B., Introduction to the Theory and Application of Differential Equations with Deviating Arguments, Academic Press. (1973)

18. Clarke, A. B., On time-dependent waiting line processes (Abst.) Ann.Math.Statist. 24, 491-492 (1953).

19. Saaty, T.L., Elements of Queueing Theory with applications , McGraw-Hill (1961)

20. Srivastava, H.M., and Kashyap, B.R.K., Special Functions in Queuing Theory, Academic Press (1982)

21. Abramowitz, M. and Stegun, I., Eds., Handbook of Mathematical Functions. Washington, D.C.: National Bureau of Standards, (1964). Reprinted by Dover Publications, New York, (1968)

22. Miller J.C.P., Bessel Functions, vol.II in Mathematical Tables, Cambridge University Press, London and New York (1952)

23. Zhang S. e Jin J., Computation of Special Functions Wiley-Interscience (1996)